Anchoring of Ammonium Cations to an 18-Crown-6 Binding Site: Molecular Mechanics and Dynamics Study

Denis Gehin,[†] Peter A. Kollman,[‡] and Georges Wipff*,[†]

Contribution from the Institut de Chimie, UA 422 du CNRS, 4 Rue B. Pascal, 67000 Strasbourg, France, and the Department of Pharmaceutical Chemistry, University of California, San Francisco, California 94143. *Received December 10, 1987*

Abstract: The complexation of ammonium cations (Am^+) by macrocyclic crown ethers and their derivatives displays interesting analogies with the recognition of substrates by receptors: selective association, flexibility of both species, and induced conformational changes upon complexation. We report results of model building, molecular mechanics, and molecular dynamics calculations on such systems. We first derive a set of atomic charges on various Am^+ ions to reproduce the gas-phase enthalpies measured for [18-6]/Am^+ complexes. In particular, we account for the sequence of stability: $MeNH_3^+ > Me_2NH_2^+ > Me_3NH^+$. Different conformations of [18-6] and anchoring modes of Am^+ are compared. For RNH_3^+ substrates, we analyze the stability of complexation for R = $MeOOC(C_6H_5)CH$, $C_6H_5CH_2$, $MeOOCCH_2$, Me, and CH_3CH_2. We find that R stabilizes the complexes mainly by attractive van der Waals interactions. We have also built derivatives of [18-6] with lateral branches (*B* = CONHMe, CO-Cys-OMe) which delineate a "cylindrical" cavity. Such substitution leads to increased binding affinity and selectivity, which we show to depend critically on the conformation of *B*. Thus, conformational changes of *B* occur upon complexation, giving an "induced fit" of the macrocycle receptor to Am^+. The calculations also demonstrate that negatively charged substituents (i.e., COO^-) on the uncomplexed face of [18-6] enhance the stability. Since such substituted [18-6] derivatives are chiral, we have tested the ability of the calculations to account for the L/D stereoselectivity for complexation of chiral Am^+ substrates. Cram's macrocycle, which displays the highest chiral recognition observed so far, has been considered first. For its L/D $MeCOO(C_6H_5)CHNH_3^+$ complexes, we calculate a preference for L over D of 1.3 kcal/mol in reasonable agreement with the experimental value of 2 kcal/mol. With [18-6] derivatives, no clear stereoselectivity is found. The molecular dynamics simulations have enabled us to demonstrate differences in flexibility not only between uncomplexed and complexed macrocycles but also among the various structural pieces of the macrocycles.

Molecular recognition in macrocyclic systems results from the complexation of a convex substance by a concave receptor. The "lock and key" complementarity between the binding sites, a result of structural and electronic features, may lead to high stability and selectivity. This is the case for the complexes of crown ethers,[1-5] spherands,[6] cyclic derivatives of urea,[7] and functionalized cyclodextrins.[8]

In addition to their very exciting properties, these "supermolecules" are interesting from a theoretical point of view. They may be used to test and develop molecular modeling techniques for larger biological systems, such as enzyme/substrate complexes, for which less experimental data are available.[9,10] In this field, much work has been devoted to the modeling of synthetic ionophores[11,12] or "artificial enzymes"[13] and to the study of the inclusion of alkali cations by spherands[14] or crown ethers[15-17] and the effect of solvation upon complexation.[18]

Among the synthetic macrocycles, crown ethers are of particular interest because they bind, with high selectivity and affinity, not only alkali cations[19] but also protonated amines.[1-5] As a step beyond first-sphere coordination compounds, crowns have been used to provide an entry into second-sphere coordination chemistry.[20]

Whereas the alkali cation complexes have been extensively studied both experimentally[21] and by molecular mechanics,[15] CNDO,[16] ab initio,[17] or Monte Carlo techniques,[18] complexes involving organic substrates have not, to our knowledge, been subjected to detailed theoretical studies using both molecular mechanics and dynamics. They are, however, important new species as models of ammonium binding receptors in biological systems. Much thermodynamic data are available both in the gas phase[22] and in solution[23-26] for these systems, and structures obtained by X-ray crystallography,[27-33] as well as detailed information gained from NMR in solution,[34] lead to a better understanding of the stability and selectivity of their associations.

The present paper is devoted to a detailed modeling study of building units which we feel essential for the recognition of ammonium substrates by 18-crown-6 (abbreviated henceforth as [18-6]) and some of its lateral derivatives depicted schematically in Figure 1.

[†] Institut de Chimie.
[‡] University of California—San Francisco.

(1) Lehn, J. M. *Struct. Bonding (Berlin)* **1973**, *16*, 1; *Pure Appl. Chem.* **1978**, *50*, 87; *Science* **1985**, *227*, 849-856.
(2) Cram, D. J.; Cram, J. M. *Acc. Chem. Res.* **1978**, *11*, 8-14. Cram, D. J. *Science* **1983**, *219*, 1977; *Angew. Chem., Int. Ed. Engl.* **1986**, *25*, 1039.
(3) Stoddart, J. F. *Chem. Soc. Rev.* **1979**, *8*, 85-142. Curtiss, W. D.; Laidler, D. A.; Stoddart, J. F.; Jones, G. *J. Chem. Soc., Perkin Trans. 1* **1977**, 1756.
(4) Prelog, V. *Pure Appl. Chem.* **1978**, *50*, 893.
(5) Kellog, R. M. *Top. Curr. Chem.* **1982**, *101*, 111-142.
(6) Trueblood, K. N.; Knobler, C. B.; Mavenk, E.; Helgeson, R. C.; Brown, S. B.; Cram, D. J. *J. Am. Chem. Soc.* **1981**, *103*, 5594.
(7) Cram, D. J.; Lam, P. Y. S.; Ho, S. P. *J. Am. Chem. Soc.* **1986**, *108*, 839-841.
(8) Bender, M. L.; Komiyama, M. In *Cyclodextrin Chemistry*; Springer-Verlag: New York, 1978; Vol. 6. Bender, M. L.; D'Souza, K. T. *Acc. Chem. Res.* **1982**, *15*, 66-72. Breslow, R. *Ibid.* **1980**, *13*, 170.
(9) Blaney, J. M.; Weiner, P. K.; Dearing, A.; Kollman, P. A.; Jorgensen, C. E.; Oatley, S. J.; Burridge, J. M.; Blake, C. C. F. *J. Am. Chem. Soc.* **1982**, *104*, 6424-6434.
(10) Wipff, G.; Dearing, A.; Weiner, P. K.; Blaney, J. M.; Kollman, P. A. *J. Am. Chem. Soc.* **1983**, *103*, 997-1005, and references therein.
(11) Pretsch, E.; Bendl, J.; Portmann, P.; Welti, M. Proceedings of the Symposium on Steric Effects in Biomolecules, Eger, Hungary, 1981; p 85.
(12) Lifson, S.; Felder, C. E.; Shanzer, A. *J. Am. Chem. Soc.* **1983**, *105*, 3866-3875.
(13) Venanzi, C. A. In *Molecular Structure and Energetics*; Liebmann, J. F., Greenberg, A., Eds.; VCH Publishers: Daytona Beach, FL, in press. Venanzi, C. A.; Bunce, J. D. *Enzyme* **1986**, *36*, 79; *Int. J. Quantum Chem., Quantum Biol. Symp.* **1986**, *No. 12*, 69.
(14) Kollman, P. A.; Wipff, G.; Chandra Singh, U. *J. Am. Chem. Soc.* **1985**, *107*, 2212.
(15) Wipff, G.; Weiner, P.; Kollman, P. A. *J. Am. Chem. Soc.* **1982**, *104*, 3249-3258.
(16) Yamabe, T.; Hori, K.; Akagi, K.; Fukui, K. *Tetrahedron* **1979**, *35*, 1065-1072.
(17) Hori, K.; Yamada, H.; Yamabe, T. *Tetrahedron* **1983**, *39*, 67-73.
(18) Ranghino, G.; Romano, S.; Lehn, J. M.; Wipff, G. *J. Am. Chem. Soc.* **1985**, *107*, 7873.
(19) Pedersen, C. J. *J. Am. Chem. Soc.* **1967**, *87*, 7017-7036. Pedersen, C. J.; Frensdorff, H. K. *Angew. Chem., Int. Ed. Engl.* **1972**, *11*, 16.
(20) Von Colquhoun, H. M.; Stoddart, J. F.; Williams, D. J. *Angew. Chem., Int. Ed. Engl.* **1986**, *98*, 483-578.
(21) Bradshaw, J. J. In *Synthetic Multidentate Macrocyclic Compounds*; Izatt, R. M., Christensen, J. J., Eds.; Academic Press: New York, 1978; Chapter 11, pp 53-109.
(22) Meot-Ner, M. *J. Am. Chem. Soc.* **1983**, *105*, 4912; *Ibid.* **1984**, *106*, 1257; *Ibid.* **1985**, *107*, 469; *Acc. Chem. Res.* **1984**, *17*, 186.

0002-7863/89/1511-3011$01.50/0

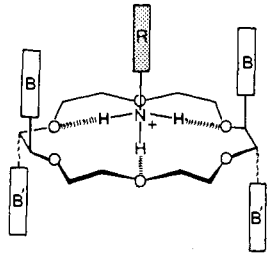

Figure 1. Schematic representation of $^{+}H_3NR$ complexes of laterally substituted 18-crown-6 ([18-6]) (from ref 37). Macrocycles considered in the calculations are as follows. **1**: $B = B' =$ H. **2**: $B =$ CONHMe, $B' =$ H. **3**: $B =$ CONHMe, $B' = COO^-$. **4**: $B =$ CONH(-L-CHCOOMe)CH_2SH (CO-Sys-OMe), $B' =$ H. Experimental structures referred to in the text are as follows. **5**: $B = B' =$ CO-Cys-OMe. **6**: $B = B' = COO^-$. **7**: $B =$ CONH(C_6H_5), $B' = COO^-$. **8**: $B = B' =$ $CONMe_2$. The $^{+}H_3NR$ substrates calculated have R = Me, Et, C_6H_5, CH_2COOMe, $CH(C_6H_5)COOMe$, $CH_2CONHCH_2COOMe$, and $CH_2CONHCH(C_6H_5)COOMe$.

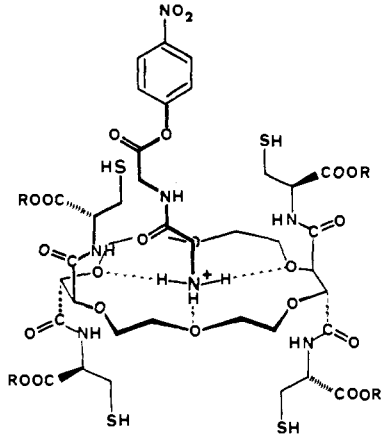

Figure 2. Schematic representation of the complex of receptor **5** with the dipeptide substrate glycylglycine *p*-nitrophenyl ester (from ref 36).

In such systems the molecular recognition extends to chemical reactions that follow the simple step first of complexation. Thus, they may be considered as artificial enzymes such as some macrocyclic derivatives of cyclodextrin,[8] urea,[7] or the Cram crown ethers[35] which mimic the serine proteases. More particularly, lateral derivatives of [18-6] have been synthetized in such a way that the reactive end groups of the receptor and the substrate may be close enough to react chemically. For instance, the tetracysteinyl macrocycle in Figure 2 not only anchors ammonium substrates to its [18-6] moiety but also catalyses the thiolysis of the *p*-nitrophenyl ester (OpNP) of the bound substrate.[36]

Similarly, in the complexes between CO-dihydro-1,4 lateral derivatives of [18-6] and pyridinium substrates anchored by a NH_3^+ binding site, an intracomplex hydride transfer is observed with a rate enhancement of 10 with respect to the rate transfer when complexation is inhibited.[37] In the same way, the tetracarboxylate derivative of [18-6], **6**, displays a strong affinity for N-protonated hydroxylamine derivatives. With the *O*-acetylhydroxylammonium ion ($CH_3COONH_3^+$), the deacylation reaction that follows complex formation is 30 times faster than acid hydrolysis of the free substrate.[38] Such reactions display interesting analogies with enzymatic catalysis: formation of a noncovalent ("Michaelis") complex anchored by a NH_3^+ binding site, followed by a catalyzed, highly selective reaction. Inhibition processes can also be monitored.[36-38]

Schematically in such systems and for complexes between ammonium (Am^+) substrates and [18-6] lateral derivatives, one may distinguish the following: (i) the *central recognition* at the anchoring site (the binding affinity decreases from primary to secondary and tertiary Am^+) and (ii) the *lateral recognition* [interaction between the lateral branches B of [18-6]$(B)_2$ and R of RNH_3^+ (Figure 1)]. With $RCHXNH_3^+$ as substrates, there may be specific interactions between X and the macrocycle (*vicinal effect*). Furthermore, when the substrate and the receptor are both chiral, *enantiomeric differentiation* may be observed upon complexation. The macrocyclic receptor of Figure 2 displays these three different types of recognition: (i) central ($^{+}$Gly-Gly-OpNP ester reacts 15 times faster than $^{+}$Pro-Gly-OpNP[36]), (ii) lateral, related to the relative side-chain lengths (ester derivatives of dipeptides react 2000 times faster than those of amino acids[36]), and (iii) enantiomeric [the dipeptide $^{+}$Gly-L-Phe-OpNP reacts 50 times faster than its D enantiomer[36]].

Our goal is to study these lateral derivatives of [18-6] as artificial enzymes and, as in a previous study of L/D peptide recognition by an enzyme,[10] to model both noncovalent Michaelis complexes between the macrocyclic receptor and ammonium substrates and transition states for the thiolysis reaction, the including several tetrahedral intermediates.

Only noncovalent complexes between the receptor and the substrates will be considered here. Models of the intracomplex reaction transition states require several mechanistic hypotheses, as well as calculation techniques able to circumvent the problem of local conformational minima (molecular dynamics). A complete conformational search for such a system, even uncomplexed, is a major task. This will be treated in a separate paper.

Here, we will analyze the structural and energetic features of the central, lateral, and chiral recognition of ammonium substrates by lateral derivatives of [18-6]. We will start from the simple uncomplexed [18-6] as a receptor, and then add lateral arms B. The site effect will be first studied with unsubstituted [18-6] and $MeNH_3^+$, $Me_2NH_2^+$, and Me_3NH^+ as substrates. This will require calibration of the atomic charges in these cations. To model the vicinal effect, we will focus on primary ammonium ions, because they lead to the most stable complexes, and vary R (R = Me, Et, $C_6H_5CH_2$, $MeOOCCH_2$-($^{+}$Gly-OMe) and MeOOC-(C_6H_5)CH-($^{+}$Gly(Phe)-OMe) (Figure 1). We will then study in more detail the $(B')_2$[18-6](B_2) derivatives, where the lateral chains B are simple CONHMe amides. This choice of B comes from their synthetic importance in functionalizing lateral derivatives of [18-6],[39] which are thus the constitutive fragments of the tetracysteinyl derivative **5** of Figure 1. With **2**, we will study the effect of $B =$ CONHMe on (i) the central recognition by comparing the $MeNH_3^+$, $Me_2NH_2^+$, and Me_3NH^+ substrates and (ii) the lateral recognition of RNH_3^+, first as a function of the conformation of B and second, for the best conformation of B, as a

(23) Izatt, R. M.; Lamb, J. D.; Izatt, N. E.; Rossiter, B. E., Jr.; Christensen, J. J.; Haymore, B. L. *J. Am. Chem. Soc.* **1979**, *101*, 6273–6276.
(24) Behr, J. P.; Lehn, J. M.; Vierling, P. *Helv. Chim. Acta* **1982**, *65*, 1852–1862.
(25) Sirlin, C. *Bull. Soc. Chim. Fr.* **1984**, *2*, 25.
(26) Peacock, S. C.; Domeier, L. A.; Gaeta, F. C. A.; Helgeson, R. C.; Timko, J. M.; Cram, D. J. *J. Am. Chem. Soc.* **1978**, *100*, 8190–8202. Helgeson, R. C.; Weisman, G. R.; Toner, J. L.; Tarnowski, T. L.; Chao, J. M.; Cram, D. J. *Ibid.* **1979**, *101*, 4928–4941.
(27) Nagano, D.; Kobayashi, A.; Sasaki, Y. *Bull. Chem. Soc. Jpn.* **1978**, *51*, 790.
(28) Trueblood, K. N.; Knobler, C. B.; Laurence, D. S.; Stevens, R. V. *J. Am. Chem. Soc.* **1982**, *104*, 1355–1362.
(29) Bovill, M. J.; Chadwick, D. J.; Sutherland, I. O.; Watkin, D. *J. Chem. Soc., Perkin Trans. 2* **1980**, 1529–1543.
(30) Daly, J. J.; Schoenholzer, P.; Behr, J. P.; Lehn, J. M. *Helv. Chim. Acta* **1981**, *64*, 1444–1451.
(31) Behr, J. P.; Lehn, J. M.; Moras, D.; Thierry, J. C. *J. Am. Chem. Soc.* **1981**, *103*, 701–703.
(32) Goldberg, I. *J. Am. Chem. Soc.* **1977**, *99*, 6049–6057.
(33) Behr, J. P.; Lehn, J. M.; Dock, A. C.; Moras, D. *Nature* **1982**, *295*, 526–527. Dock, A. C.; Moras, D.; Behr, J. P.; Lehn, J. M. *Acta Crystallogr.* **1983**, *C39*, 1001.
(34) Live, D.; Chan, S. I. *J. Am. Chem. Soc.* **1976**, *98*, 3769. Dale, J.; Kristiansen, P. O. *Acta Chem. Scand.* **1972**, *26*, 1741.
(35) Cram, D. J.; Sogah, G. D. Y. *J. Chem. Soc., Chem. Commun.* **1981**, 625–628.
(36) Lehn, J. M.; Sirlin, C. *J. Chem. Soc., Chem. Commun.* **1978**, 949–951. Lehn, J. M.; Sirlin, C. *Nouv. J. Chim.* **1987**, *11*, 693.
(37) Behr, J. P.; Lehn, J. M. *Helv. Chim. Acta* **1980**, *63*, 2112–2118.
(38) Lehn, J. M.; Nishiya, T. *Chem. Lett.* **1987**, 215–218.
(39) Girodeau, J. M.; Lehn, J. M.; Sauvage, J. P. *Angew. Chem., Int. Ed. Engl.* **1975**, *14*, 764.

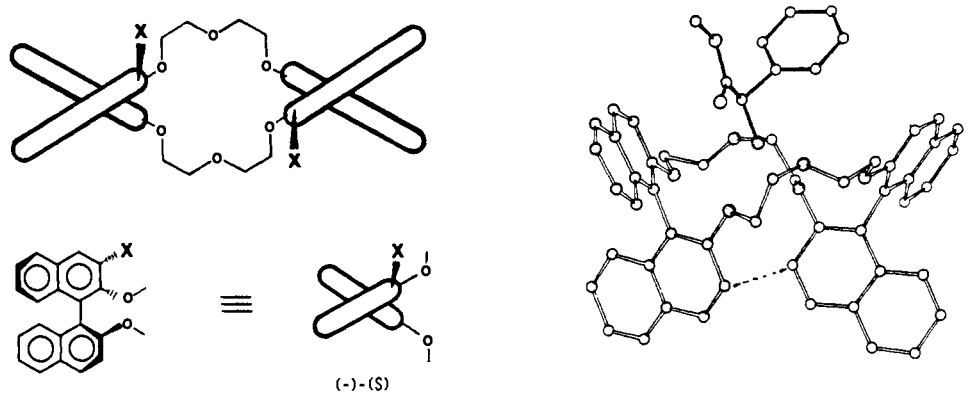

Figure 3. Cram chiral (*S,S*) receptors **9a** and **9b** (from ref 26 and 32). **9a** (left) X = Me. Schematic representation of the receptor considered in the calculations. **9b** (right) X = H. The receptor in its complex with PF_6^-, $^+H_3NCH(C_6H_5)COOMe$ (X-ray structure).

function of R (R = alkylammonium, ester derivatives of protonated amino acids, and dipeptides). With $^+$Pro-OMe as the substrate, we will specifically model the central and lateral recognition coupling effect on the complexation of N-substituted amines. With the chiral receptor **2**, we will also test by computation the ability of chiral recognition toward L/D ammonium substrates and compare the complexes formed with the L/D ester derivatives of phenylglycine ($^+$Gly(Phe)-OMe) and glycylphenylalanine ($^+$-Gly-Phe-OMe). The chiral recognition upon complexation involves small energy differences, and there is no experimental evidence of such an effect for **2** and the above chiral substrates. On the other hand, the enantiomeric discrimination observed in the thiolysis of $^+$Gly-Phe-OpNP is weak and occurs probably in the transition state, rather than at the noncovalent complexation step.[10,25] We therefore felt it important to test our computational procedure on another parent system, Cram's chiral macrocycles **9a** and **9b** (Figure 3), which have also six ether sites and bind ammonium substrates.[26] In its (*S,S*) conformation, **9a** complexes selectively the L enantiomer of phenylglycine methyl ester ($^+$-Gly(Phe)-OMe) compared with the D ($\Delta\Delta G$ = 2 kcal/mol in chloroform[26]).

In addition to applying molecular mechanics to the above systems, we applied molecular dynamics to study conformational flexibility and heterogeneity.

Computational Technique

We use a simple molecular mechanics approach with the software package AMBER (Assisted Model Building and Energy Refinement[40]) to calculate the energy and optimize the structures. The total energy E_t has the following form:

$$E_t = \sum_{\text{bonds}} K_r(r - r_{eq})^2 + \sum_{\text{angles}} K_\theta(\theta - \theta_{eq})^2 + \sum_{\text{dihedrals}} \frac{V_n}{2}[1 + \cos(n\phi - \gamma)] + \sum_{i<j}\left[\frac{A_{ij}}{R_{ij}^{12}} - \frac{B_{ij}}{R_{ij}^{6}} + \frac{q_i q_j}{\epsilon R_{ij}}\right] + \sum_{\text{H bonds}}\left[\frac{C_{ij}}{R_{ij}^{12}} - \frac{D_{ij}}{R_{ij}^{10}}\right]$$

where r, θ, and ϕ represent, respectively, the bond length, the bond angle, and the dihedral angle. R_{ij} is the distance between atoms i and j, q_i the atomic charge on i, and ϵ the dielectric constant. The deformations of bonds r and bond angles θ from their reference values r_{eq} and θ_{eq} are treated in the harmonic approximation, and the rotation around dihedral angles is taken into account. The interactions between [18-6] and ammonium ions, Am^+, and those between nonbonded atoms are represented by a 1-6-12 potential. There are thus no explicit terms for polarization and charge transfer, but this can be almost completely compensated for by an appropriate choice of electrostatic term.[41] The summation of the nonbonded interactions runs over all atom pairs i and j separated by at least three bonds. As in previous calculations on crown ethers and cryptates,[15,42] we take the dielectric constant ϵ equal to 1, and the 1-4 Van der Waals interactions are divided by 2. The CH, CH_2, and CH_3 groups are treated in the united atom approximation.[43]

For the amino acid fragments, we use the parameters of Weiner et al.,[43] with charges fitted on electrostatic potentials, but for CONHMe, we also tested an alternative set of charges resulting from ab initio calculations. For the [18-6] fragment, we used the same force field as in ref 15, with charges $q_0 = -0.30$ and $q_{CH_2} = 0.15$, which account for the dipole moment of dimethyl ether in the gas phase.

For the Cram's macrocycle, we added to the force field of [18-6], a V_2 torsional term of 10 kcal/mol for O-C(sp^2)-C(sp^2)-C(sp^2) and of 0 kcal/mol for the X-C(naphthyl)-C(naphthyl)-X dihedral angles as used for calculations on spherands.[14] We kept the charges on the cycle as close as possible to those used for [18-6], with $q_0 = -0.3$ and $q_{CH_2} = 0.15$. The charges of the remaining atoms of the naphthyls were set to zero.

For the ammonium site we choose to calibrate the atomic charges to reproduce the experimental gas-phase complexation enthalpies between [18-6] and $MeNH_3^+$ (-46 kcal/mol[22]), and Me_3NH^+ (-41 kcal/mol[22]). These charges are then used for the other ammonium sites (in N-protonated amino acids and dipeptides).

In most cases, the geometry has been fully relaxed toward the nearest local minima until the RMS of the energy gradient was smaller than 0.05 kcal/mol, or the energy lowering per cycle was smaller than 10^{-6} kcal/mol. In some cases, we also performed a partial optimization, keeping part of the system rigid in order to study structures away from their local minima.

The total energy obtained by molecular mechanics has no absolute meaning. Only two systems of the same type calculated in the same conditions can be compared directly. In order to compare the stabiilties of different complexes, we define the complexation energy E_c as the difference between the total energy of the complex and the total energy of the receptor and substrate in their most stable conformation calculated under the same conditions. Because of the deformation energy induced by complexation, E_c may be larger than the interaction energy E_{int} within the complex. E_{int} may be analyzed further by considering the constituent parts of the receptor (the [18-6] moiety, the lateral arms *B*, piece by piece) and of the substrate (NH_3^+, NH_2^+, NH^+, and R in RNH_3^+).

On many of these systems, molecular dynamics simulations were carried out with the program AMBER 2.0.[40] Starting from the optimized structures with random velocities, we carried out these dynamic simulations at a temperature of 300 K for 50 ps using a time step of 1 fs.

Choice of Starting Geometries. Several X-ray structures of unsubstituted [18-6], as well as of tetrasubstituted lateral derivatives, are available. There is, however, no structure for simple disubstituted derivatives either free or complexed by ammonium substrates.

The [18-6] macrocycle is very flexible and takes up different conformations depending on its environment and that of the complexed cation.[18,27-33,35,39,44,45] The uncomplexed crown is of C_i symmetry with no cavity,[15,31,39] whereas the D_{3d} conformation is found in complexes with NH_4^+,[27] $MeNH_3^+$,[28] benzylammonium ($C_6H_5CH_2NH_3^+$),[29] and in molecular environments involving polar OH, NH, or CH bonds.[18,27-33,39] Such a C_3 symmetry is, however, not compatible with two lateral substituents in the syn diaxial arrangement of $(B')_2$[18-6]$(B)_2$, which is, at best, of C_2 symmetry. The D_{3d} and C_2 conformers of the crown are thus considered as typical forms of unsubstituted and syn disubstituted [18-6],

(40) Weiner, P. K.; Kollman, P. A. *J. Comput. Chem.* **1981**, *2*, 287. Singh, U. C.; Weiner, P.; Caldwell, J.; Kollman, P. A. AMBER 2.0, U. C.—San Francisco, 1985.
(41) Hayes, D. M.; Kollman, P. A. *J. Am. Chem. Soc.* **1976**, *98*, 3335-3345.
(42) Wipff, G.; Kollman, P. A. *Nouv. J. Chim.* **1985**, *9*, 457.
(43) Weiner, S. J.; Kollman, P. A.; Case, D. A.; Chandra Singh, U.; Ghio, C.; Alagona, G.; Profeta, S.; Weiner, P. *J. Am. Chem. Soc.* **1984**, *106*, 765-784.
(44) Dale, J. *Isr. J. Chem.* **1980**, *20*, 3, and references therein.
(45) Dobler, M. *Chimia* **1984**, *38*, 415-421.

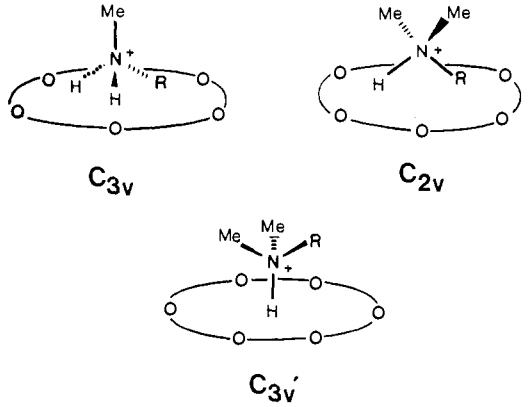

Figure 4. Schematic representation of the ammonium anchoring modes C_{3v} (R = H for $MeNH_3^+$, R = Me for $Me_2NH_2^+$), C_{2v}, and $C_{3v'}$ (R = H for $Me_2NH_2^+$, R = Me for Me_3NH^+) to [18-6].

and their ability to bind ammonium cations has to be compared.

For unsubstituted [18-6], the C_2 conformation has been taken from the complex between $H_3^+NCH_2CH_2NH_3^+$ and the tetracarboxylate derivative **6** of [18-6] (Figure 1). The O-C-C-O dihedral angles are successively $g^+g^-g^-g^+g^-g^-$ instead of $g^+g^-g^+g^-g^+g^-$ in the D_{3d} conformer.

The structure of the lateral amide derivative **2** [[18-6](CONHMe)$_2$ (B = CONHMe, B' = H; Figure 1)], has been taken from the $SrCl_2$ complex of **7** (Figure 1), where we have replaced the phenyl by a methyl group.

In the complexes with $MeNH_3^+$, $Me_2NH_2^+$, and Me_3NH^+, several typical arrangements of the cation above the D_{3d} and C_2 crowns have been considered. They are refered to as C_{3v}, C_{2v}, and $C_{3v'}$ (see Figure 4).

For primary ammonium ions, this arrangement is presumably C_{3v} as observed for various RNH_3^+/[18-6] complexes.[27-29] For $Me_2NH_2^+$ and Me_3NH^+ complexes, no X-ray structures are available, but a C_{2v} or $C_{3v'}$ position of the cation may be expected, as this leads to a compromise between the anchoring of NH^+ and the Me/cycle steric repulsion.

For the Cram macrocycle and its chiral ammonium complexes, we have started from the X-ray structure of the complex with the methyl ester of D-phenylglycine [D-$^+$Gly(Phe)-OMe; see **9b** in Figure 3] and have added methyl substituents to the naphthyl groups. The L substrate has been obtained from the D by exchange of the C_6H_5 and COOMe groups. Different positions of the L and D substrates in the macrocycle have been considered by rotations of 60, 120, 180, 240, and 300°/around the C-NH_3^+ axis. Thus, we considered six different starting geometries for each enantiomer.

The dipeptides substrates, for which no structures are available, have been built with AMBER in extended conformations of the main chain as depicted in Figure 2. Such a conformation leads to a close proximity of the reactive ester groups of the substrate with the thiol of the receptor in that system and has been kept for more simple analogues studied as well.

The ammonium complexes have then been assembled graphically with the software FRODO on the PS300 picture system.[46] We started with a perched position of Am^+ over the macrocycle[27-29] and in the cavity delineated by the lateral arms of the receptor. A two-step optimization procedure was performed: first the macrocycle was constrained to its starting coordinates C_0 by using a restraint energy [$E_r = K_r(C_0 - C)^2$, K_r = 10 kcal/mol], and the position of the ammonium was relaxed in order to avoid artificially large energy gradients; then the coordinates of the whole system were fully relaxed.

Results

(A) Ammonium Complexes of Unsubstituted [18-6]. Our purpose in this section is first to calibrate atomic charges on primary, secondary, and tertiary ammonium ions and to compare different anchoring modes for these cations. Second, we will study the vicinal effect in RNH_3^+ substrates in order to determine, in the absence of lateral substituents, the effect of R upon complexation. Finally, we will move RNH_3^+ out of its optimized position and assess its mobility within the complexes.

(1) Atomic Charges on NH_3^+, NH_2^+, and NH^+. Structure of the Complexes with [18-6]. We have chosen to calibrate these charges to take into account the interactions in the gas phase between $MeNH_3^+$ and [18-6] (-46 kcal/mol[22]), rather than between $MeNH_3^+$ and a single ether site (-22 kcal/mol[22]). These experimental values (Table I and ref 22) clearly demonstrate the nonadditivity of ammonium/ether interactions in polyethers due to charge distribution and geometry effects.

Table I. Experimental Gas-Phase Dissociation Enthalpies ΔH^a and Calculated Complexation Energy E_c^a of Ammonium/Ligand Complexes

	ammonium		
	$MeNH_3^+$	$Me_2NH_2^+$	Me_3NH^+
q_{Me}[b]	0.05	0.12	0.16
q_H	0.25	0.21	0.17
q_N	0.20	0.34	0.35
ligand:			
OH_2			
ΔH	-16.8	-15.0	-14.5
OMe_2			
ΔH	-22.0		-19.5
E_c	-9.9	-8.3	-7.9
[18-6]			
ΔH	-46.0		-41.0
E_c	-46.1	-43.7	-39.0

[a] ΔH and E_c in kcal/mol. [b] Atomic charges on ammonium.

Thus, a charge calibration on the $MeNH_3^+/OMe_2$ complex would lead to a overestimate of the interactions in the $MeNH_3^+$/[18-6] complex, as shown in Table I.

The complexed macrocycle should be more polarized than the free macrocycle. We have, however, kept the same charges in both cases (q_O = -0.3, q_{CH_2} = 0.15) and taken the charges of ref 15 in order to make comparison possible between these two situations. We performed several test calculations on a more polarized cycle with several charge distributions in $MeNH_3^+$ which led to complexation energies E_c much larger than the experimental -46 kcal/mol. For example, with q_O = -0.4 and q_{CH_2} = 0.2 on the macrocycle and q_N = 0.2 and q_H = 0.25 for $MeNH_3^+$, we calculated E_c = -63.7 kcal/mol for the "D_{3d}" complex. An alternative procedure to compensate for this excessively large energy would be to decrease the total charge on $MeNH_3^+$, similar to the charge reduction used to model Zn^{2+} complexes.[47] We preferred, however, to keep a total charge 1+ on all ammonium substrates.

From $MeNH_3^+$ to Me_3NH^+, we reduce part of the positive charge on the alkyl groups rather than on H, which is less polarizable than Me. For $Me_2NH_2^+$, no gas-phase data are available, and we take charges intermediate between those of $MeNH_3^+$ and Me_3NH^+.

We have also performed test calculations using a 10-12 potential for hydrogen-bonded atoms (C and D parameters of the above formula) with several sets of charges and found an excessively large complexation energy for $MeNH_3^+$/[18-6] (-62.5 kcal/mol with q_N = 0.20, q_H = 0.25 and C = 6525, D = 2500). This is why we kept a simple 1-6-12 potential for the Am^+/crown interactions.

The optimized atomic charges are reported in Table I with the corresponding complexation energies E_c. Note that for $MeNH_3^+$, $Me_2NH_2^+$, and Me_3NH^+ all atoms are positively charged, with q_{Me}, q_N, and q_H close to the values proposed by Hudson et al. for molecular mechanics calculations[48] and to those obtained from CNDO/2.[49] Such a distribution differs, however, from the results of ab initio calculations, where q_N is negative.[50] We have found that with q_N negative and q_H more polarized, E_c for $MeNH_3^+$/[18-6] is overestimated.

With the charges given in Table I, the complexation energies E_c for the [18-6] complex are in excellent agreement with ex-

(46) Jones, T. A. *Comput. Crystallogr.* **1982**, 303. Pflugrath, J. W.; Saper, M. A.; Quichio, P. A. *J. Mol. Graphics* **1983**, *1*, 53.

(47) Vedani, A.; Dobler, M.; Dunitz, J. O. *J. Comput. Chem.* **1986**, *7*, 701-710.

(48) Abraham, R. J.; Hudson, B. *J. Comput. Chem.* **1985**, *6*, 173-181.

(49) Aue, D. H.; Webb, H. M.; Bowers, M. T. *J. Am. Chem. Soc.* **1976**, *98*, 311-317.

(50) Hagler, T.; Lapiccirella, A. *Biopolymers* **1976**, *15*, 1167-1200.

(51) Lifson, S.; Hagler, A. T.; Dauber, P. *J. Am. Chem. Soc.* **1979**, *101*, 5111-5121.

Table II. Energies[a] and Geometries of [18-6]/Ammonium Complexes: The Site Effect

	ammonium		
	$MeNH_3^+$	$Me_2NH_2^+$	Me_3NH^+
[18-6][b]	D_{3d}	C_2	C_2
[18-6][c]	C_{3v} or C_2	C_{3v}, C_2, or $C_{3v'}$	$C_{3v'}$ or C_2
[18-6][d]	C_{3v}	C_2	$C_{3v'}$
E_t[e]	8.5	12.3	15.9
E_c[f]	−46.1	−43.7	−39.0
ΔE_c[g]	0.0	2.4	7.1
E_{int}[h]	−46.3	−45.0	−40.0

[a] Energies in kcal/mol. [b] Conformation of the crown in the most stable complex. [c] Type of anchoring of the ammonium before optimization. [d] Type of anchoring after optimization (see Figure 4). [e] Total energy. [f] Complexation energy (see text). [g] Change in complexation energy relative to $MeNH_3^+$. [h] [18-6]/ammonium interaction energy within the complex.

perimental values for $MeNH_3^+$ (−46.1 kcal/mol) and very satisfactory for Me_3NH^+ (−39.0 kcal/mol). In particular, we obtain the same order of stability essential for the central recognition: $NH_3^+ > NH_2^+ > NH^+$.[23-25]

Interestingly, the results of Table II, and analysis on the graphic system, show that the relative binding of primary/secondary/tertiary ammonium ions depends not only on the number and magnitude of $NH^+\cdots O$ interactions but also on the positioning of the cation over the macrocycle and on the conformation of the cycle. Indeed, depending on the nature of Am^+, either the "D_{3d}" or "C_2" conformation of the cycle is preferred. The $MeNH_3^+$ complex is slightly more stable for "D_{3d}" than "C_2" (ΔE_c = 0.8 kcal/mol), in agreement with the available X-ray structures.[27-29] For the secondary and tertiary ammonium ions, the most stable complexes have a "C_2" macrocycle (preferred by 2 and 1 kcal/mol, respectively, for $Me_2NH_2^+$ and Me_3NH^+, compared with the "D_{3d}" complexes). The primary ammonium ion is anchored by three linear $NH\cdots O$ hydrogen bonds (C_{3v} position, see Figure 4) with three oxygen atoms pointing up toward the substrate. The average of the six $NH^+\cdots O$ distances is slightly longer in the "D_{3d}" (2.25 Å) than in the "C_2" form (2.17 Å). The secondary ammonium $Me_2NH_2^+$ is perched over the "C_2" macrocycle, anchored by four bifurcated H bonds (C_{2v} disposition, see Figure 4) with $NH^+\cdots O$ and $N\cdots O$ distances similar to those found in the "C_2" complex of $MeNH_3^+$. The tertiary ammonium prefers the $C_{3v'}$ disposition over the "C_2" cycle. The NH^+ points inside the cavity approximately along the C_2 axis of the crown and has no possibility to be anchored by bifurcated H bonds, but only by six electrostatic interactions with the ether oxygens, with no directional character.

The analysis of the energy components shows that the complex stability results from a compromise between the conformational energy of [18-6] within the complex and the interaction energy E_{int} with Am^+. In the various complexes, the [18-6] moiety is slightly more stable "D_{3d}" than "C_2" (56 and 57.5 kcal/mol), as in the free crown (54.6 and 56 kcal/mol). On the other hand, E_{int} is better for the "C_2" than for the "D_{3d}" crown with each of the three ammonium ions (by 0.7, 3.1, and 1.8 kcal/mol, respectively, for $MeNH_3^+$, $Me_2NH_2^+$, and Me_3NH^+). As a result, the "D_{3d}" and "C_2" complexes have a comparable stabiity for primary and tertiary Am^+. With $Me_2NH_2^+$, however, the complex is slightly more stable for "C_2" than for "D_{3d}".

(2) [18-6]/RNH_3^+ Complexes: Effect of α-Substituents on the Recognition of RNH_3^+ (the Vicinal Effect). We wish here to compare the stability of complexes between unsubstituted [18-6] and primary Am^+ as a function of RNH_3^+ for R = Et, $MeOOCCH_2$-(+Gly-OMe), $C_6H_5CH_2$, $MeOOC(C_6H_5)CH$-(+Gly(Phe)-OMe) (Figure 1). The results in Table III show that for R = Me and Et, the complexation energies are comparable. This is in agreement with the fact that $MeNH_3^+$ and $C_6H_{11}NH_3^+$ have the same complexation energy with [18-6] in the gas phase[22] and therefore indicates that the alkyl chain does not interact significantly with the cycle. For the other substituents, we calculate an increased stability of the complex (by 4–9 kcal/mol) caused mainly by Van der Waals interactions within the complex.

Table III. Complexes between [18-6]$(CONHMe)_2$ and $MeNH_3^+$ with Three Typical Conformations of the Lateral Chains

	set of charges					
	SET1[a]			SET2[b]		
	$(H_t,H_f)^{+c}$	$(H_t,O_f)^{+c}$	$(O_t,O_f)^{+c}$	$(H_t,H_f)^{+c}$	$(H_t,O_f)^{+c}$	$(O_t,O_f)^{+c}$
E_t[d]	−8.5	−19.1	−22.0	−18.2	−29.4	−40.9
E_c[d]	−36.4	−47.0	−50.1	−32.2	−48.3	−54.5
ΔE_c[e]	9.8	−0.8	−3.9	14.0	−2.1	−8.2
E_{rec}[f]	28.4	31.4	40.2	14.9	20.7	28.1
E_{int}[d]	−36.9	−50.5	−62.2	−33.1	−50.1	−69.0

[a] Atomic charges on CONHMe from ref 50: q_C, 0.290; q_O, −0.290; q_{Me}, 0.160; q_H, 0.210; q_N, −0.370. [b] Atomic charges on CONHMe from ref 43: 0.626, −0.500, 0.146, 0.248, −0.520, respectively. [c] CONHMe conformation. See text and Figure 7. Characterizes whether NH or C=O, in each branch, points inside the cavity. [d] See definitions in Table II. [e] Change in complexation energy brought about by the lateral CONHMe substituents ($\Delta E_c = E_c - E_c$([18-6]/$MeNH_3^+$ complex). [f] Energy of the "receptor" [18-6]$(CONHMe)_2$ within the complex.

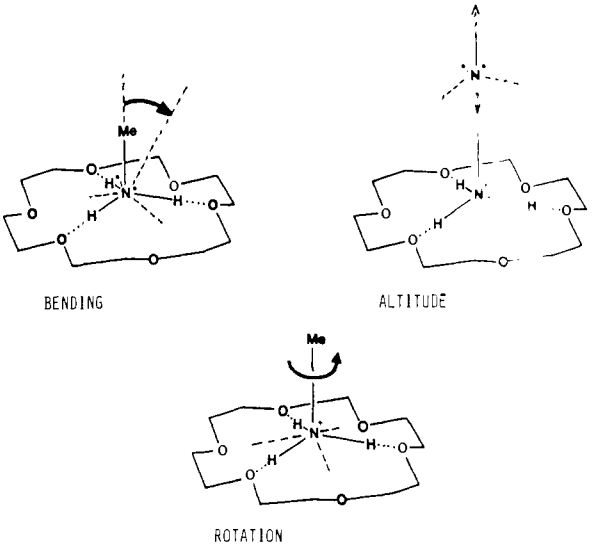

Figure 5. Schematic representation of the ^+H_3N mobility as a function of (a) the ^+H_3N–C bending, (b) the altitude of ^+H_3N above the [18-6] cycle, and (c) the rotation about the ^+H_3N–C bond.

Compared with Me, each of the vicinal substituents C=O and C_6H_5 brings a stabilization of ~4 kcal/mol, which is additive in the complexes with +Gly(Phe)-OMe.

The NH_3^+/cycle interactions remain close to −46 kcal/mol in these different complexes, despite perturbation in the anchoring of $C-NH_3^+$ resulting from interactions between the vicinal substituents in R and the cycle. As a result of these interactions, the $C-NH_3^+$ axis, perpendicular to the cycle when R = Me and Et, becomes slightly bent with R = $C_6H_5CH_2$, $MeOOCCH_2$, and $MeOOC(C_6H_5)CH$ (Figure 5a). One also notices that the altitude of nitrogen over the cycle (0.65 and 0.63 Å for the two alkyl substituents) increases with bulkier R (by 0.10, 0.15, and 0.18 Å, respectively). The bent position of $C-NH_3$ is similar to that found in the X-ray structure of the benzylammonium thiocyanate complex of [18-6].[29]

In order to evaluate the energy involved in such repositioning, we have taken these optimized structures and constrained the C–N axis to be perpendicular rather than bend (see Figure 5a). We find only a small destabilization (0.8 kcal/mol), which indicates that the anchoring is quite flexible. In the next section, other aspects of the mobility of NH_3^+ over the cycle are reported.

(3) Mobility of the Anchoring of NH_3^+ over the [18-6] Cycle. We wished to model and test two other aspects of the NH_3^+ mobility within the complexes. The first is to change the "altitude" of nitrogen over the cycle (see Figure 5b). This is important because in the intracomplex reaction (i.e., thiolysis of Figure 2 or hydride transfer) "vertical" mobility may facilitate a correct positioning of functional groups of the receptor with respect to those of the substrate, leading to increased catalysis. Because the

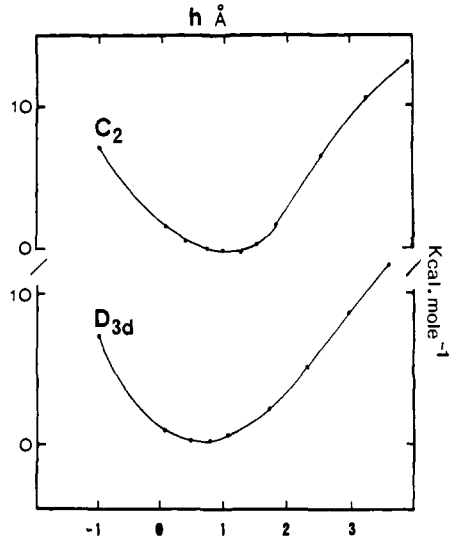

Figure 6. Mobility of $^{+}H_3NMe$ anchored to the C_2 (above) and D_{3d} (below) conformers of [18-6]: energy as a function of the "altitude" of nitrogen above the cycle (see Figure 5b).

interactions in Am^+/[18-6] depend mainly on the NH_3^+/cycle orientation, we chose to move $MeNH_3^+$ over the "D_{3d}" and "C_2" cycles.

In order to keep all the structures from converging toward the same minimum, we constrained the cation at different altitudes over the cycles (with a restraint force constant of 50 kcal/mol) to calculate the energies reported in Figure 6.

The results show that the complex with the cation inside the crown still has considerable internal flexibility. Indeed, a vertical displacement of 0.5 Å from the equilibrium position costs less than 1 kcal/mol for the "C_2" complex and 0.5 kcal/mol for the "D_{3d}" complex.

The second aspect of the mobility concerns the rotation around the C–NH_3^+ bond (see Figure 5c). Indeed, in our optimized "D_{3d}" complexes, as in the X-ray structures of [18-6] complexed with NH_4^+,[27] $MeNH_3^+$,[28] and $C_6H_5CH_2NH_3^+$,[29] three linear NH···O H bonds with three oxygen atoms pointing up are observed. A rotation of 60° around C–N would decrease these interactions, but would lead to better electrostatic interactions with the other three oxygen atoms pointing down (Figure 5b). We have thus considered the "D_{3d}" and "C_2" complexes and rotated NH_3^+ above the cycle at constant altitude in order to assess the strength of linear NH···O H bonds over nonlinear ones. A very low energy barrier (0.3 kcal/mol) is obtained in the two cases. The inclusion of polarization, charge transfer having more directional character, would increase this barrier. However, our calculations demonstrate that there is no significant electrostatic barrier for this rotation. Furthermore, since the "D_{3d}" and "C_2" complexes are very close in energy, they should be in rapid equilibrium.

Molecular dynamics simulations were carried out for the free and $MeNH_3^+$ complexed [18-6] in both D_{3d} and C_2 conformations. In free [18-6], both C_2 and D_{3d} simulations remained in the conformational region they began for the entire 50 ps, with rms fluctuations of O–C–C–O dihedrals of 10° and average rms atom motions of 0.45 Å (C_2) and 0.70 Å (D_{3d}).

In the $MeNH_3^+$-complexed simulations, there is a significant decrease in the rms fluctuation of the crown, to 0.36 Å (C_2) and 0.30 Å (D_{3d}). During both of these simulations, the NH_3^+ group spins around its pseudo C_3 axis. The average N···O distance is 3.1 Å in both simulations, with a rms motion of 0.2 Å, compared to the average distance of 3.0 Å in the minimized structures.

(B) Lateral Amide Derivatives of [18-6]. Our aim in this section is first to get some insight into the conformation of the lateral amide fragments in the free receptor **2** (B = CONHMe, B' = H; Figure 1) and in its $MeNH_3^+$ complex and to perform a detailed conformational analysis of this unit, which may or may not delineate a cavity depending on its conformation. Incidentally, we will assess the effect of simplification (going from a tetra-substituted receptor to a disubstituted one) by comparison of the $MeNH_3^+$ complexes of the tetrasubstituted receptor **3** (with B = CONHMe, B' = COO^-; Figure 1) with those of the disubstituted crown **2**.

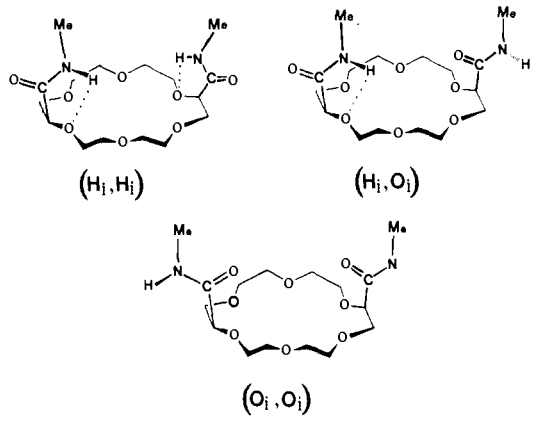

Figure 7. Typical orientations of the CONHMe branches in [18-6]-$(CONHMe)_2$. The amide is trans. ϕ_1' and ϕ_1 correspond to the O_{cycle}–C–C–N dihedral angles of the left and right lateral branches, respectively. Values of (ϕ_1', ϕ_1) optimized with SET2 are (30°, 30°) in (H_i,H_i), (30°, 230°) in (H_i,O_i), and (230°, 230°) in (O_i,O_i). SET1 leads to identical values (with a few degrees). Values in experimental structures are (17°, 19°) for receptor **7** and (215°, 218°) for receptor **8**.

The second important point will be to analyze the effect of lateral substituents (CONHMe) on the central recognition (primary/secondary/tertiary Am^+) and on lateral recognition (comparison of ester derivatives of amino acids and dipeptides). Moving to more complex systems, we wish then to have further insight into lateral recognition by changing B from CONHMe to the cysteinyl derivative **4** (see Figure 1; B = CO-Cys-OMe, B' = H) with different dipeptides as substrates.

(1) Conformation of the Lateral CONHMe Chains in the Uncomplexed Receptor [18-6](CONHMe)$_2$. This conformation depends on the O_{cycle}–C–C–N dihedral angles (ϕ_1 and ϕ_1'; see Figure 7), which connect the cycle with the chains, and on the conformation of the amide O=C—N—H fragment.

We first analyzed the conformation of one chain (B) of [18-6](B)$_2$, keeping the other fixed, and then we considered different conformations for the second chain.

We started with the conformation of the amides and of the crown in the $SrCl_2$ complex of **7** (see Figure 1), where the amide is trans (O=C—N—H = 177°) and ϕ_1 = 14°, so that each N—H is hydrogen bonded to one ether oxygen of the cycle (see Figure 7). ϕ_1 has been rotated by 360° in increments of 20°, and the structures were optimized in two ways: first, by constraining ϕ_1 (with a restraint constant of 10 kcal/mol/Å^2) in order to calculate the energy profile and the rotational barriers (Figure 8) and, second, without any constraint to obtain the energy minima. These calculations were performed with two sets of charges on CONHMe: the first set, SET1, with small polarity, comes from Mulliken populations of STO3G ab initio calculations on *N*-methylacetamide;[50] SET2, from Weiner et al., is more polar and has been fitted on electrostatic potential surfaces.[43] They are reported in Table IV.

The two procedures lead to two minima (H_i,H_i), (H_i,O_i) which can be characterized by the NH or C=O orientations inside the cavity of the macrocycle (see Figure 7).

The full optimization starting with $-90° > \phi_1 > 80°$ converged to (H_i,H_i), whereas (H_i,O_i) (ϕ_i = 230°) was obtained with $180° > \phi_1 > 260°$. The optimized conformer (H_i,H_i) is more stable than (H_i,O_i) by 6.5 kcal/mol (charges of SET1) or 5 kcal/mol (charges of SET2).

The energy barrier between these two forms is 8.5 kcal/mol (see Figure 8) or 10.0 kcal/mol, respectively, with SET1 and SET2.

Next, we changed the conformation of the second CONHMe chain, starting from the unsymmetrical (H_i,O_i) conformer, and rotated ϕ_1' (O_{cycle}–C–C–N angle). Again, two marked energy

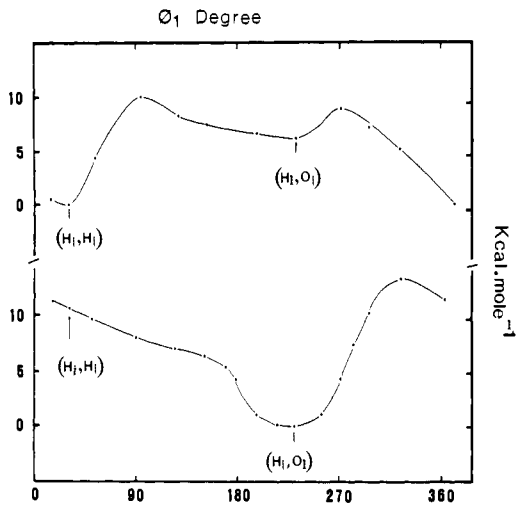

Figure 8. Energy profile for the rotation of O_{cycle}–C–C–N (ϕ_1) in one lateral arm of [18-6](CONHMe)$_2$/MeNH$_3^+$ at infinite separation (top) and with MeNH$_3^+$ fixed at 4.5 Å above the mean plane of the ring (bottom). The amide is trans and the second lateral arm remains in its H_i starting conformation (see Figure 7). Calculations are done with atomic charges of SET2.

Table IV. Complexes between [18-6](CONHMe)$_2$ and MeNH$_3^+$ with Three Typical Conformations of the Lateral Chains

	set of atomic charges					
	SET1[a]			SET2[b]		
	$(H_i,H_i)^{+c}$	$(H_i,O_i)^{+c}$	$(O_i,O_i)^{+c}$	$(H_i,H_i)^{+c}$	$(H_i,O_i)^{+c}$	$(O_i,O_i)^{+c}$
E_t[d]	−8.5	−19.1	−22.0	−18.2	−29.4	−40.9
E_c[d]	−36.4	−47.0	−50.1	−32.2	−48.3	−54.5
ΔE_c[e]	0.0	−10.6	−13.5	0.0	−11.2	−22.7
δE_c[f]	9.7	−0.9	−4.0	13.9	−2.2	−8.3
E_{rec}[g]	28.4	31.4	40.2	14.9	20.7	28.1
E_{int}[d]	−36.9	−50.5	−62.2	−33.1	−50.1	−69.0

[a] Atomic charges on CONHMe from ref 50: q_C, 0.290; q_O, −0.290; q_{Me}, 0.160; q_H, 0.210; q_N, −0.370. [b] Atomic charges on CONHMe from ref 43: 0.626, −0.500, 0.146, 0.248, −0.520, respectively. [c] CONHMe conformation. See text and Figure 7. Characterizes whether NH or C=O, in each branch, points inside the cavity. [d] See definitions in Table II. [e] Complexation energy relative to that of the $(H_i,H_i)^+$ complex. [f] Change in complexation energy brought about by the lateral CONHMe substituents ($\delta E_c = E_c - E_c$([18-6]/MeNH$_3^+$ complex). [g] Energy of the "receptor" [18-6](CONHMe)$_2$ within the complex. The energy of the [18-6] moiety is fairly constant (58 kcal/mol).

minima are obtained: (H_i,O_i) is more stable than (O_i,O_i) (ΔE = 6 and 7 kcal/mol with SET1 and SET2 respectively). The barrier from (H_i,O_i) to (O_i,O_i) is the same as from (H_i,H_i) to (H_i,O_i), which indicates that the two CONHMe chains have no noticeable interaction. To summarize the results so far, the preferred conformation of the CONHMe lateral arms of [18-6] in the "gas phase" and in the absence of molecular environment is the same as in the $SrCl_2$ complex of the $CONHC_6H_5$ derivative 7.[30]

The energy component analysis shows that, upon rotation of CONHMe, the energy of [18-6] and of CONHMe are fairly constant. Their interaction energy, however, mainly electrostatic, changes significantly and parallels the total energy. In particular, (H_i,H_i) is stabilized by NH···OCH_2 bonds, whereas (O_i,O_i) has repulsive CONHMe/cycle interactions.

The second parameter that determines the conformation of the lateral arms is the amide O=C—N—H angle (ϕ_2). For the isolated O=C—NHMe fragment, we calculated a rotation barrier of 17 kcal/mol, in agreement with the 19 kcal/mol given by ab initio calculations on *N*-methylacetamide,[51] and the cis and trans planar forms have nearly the same energy. We have rotated the O=C—NHMe bond in the (H_i,H_i) and (H_i,O_i) macrocycles from trans to cis, in increments of 20°, and fully optimized the structures that became planar: cis when we started with $-90° > \phi_2 > 90°$ and trans with $90° > \phi_2 > 270°$. For (H_i,H_i), the trans form was much more stable than cis with the two sets of charges (10 and 8.5 kcal/mol, respectively), whereas for (H_i,O_i) cis and trans have similar energies.

Where does this cis/trans energy difference come from? Again, we find that it mostly results from electrostatic cycle/CONHMe interactions (−8.5 and −0.7 kcal/mol, respectively, for cis and trans) and the loss of the NH···OCH_2 hydrogen bond when the amide is cis. We have not calculated the rotation barrier around O_{cycle}–C–C–N when the amide is cis instead of trans, but have checked on the computer graphics system that no stable form could be thus obtained, due particularly to the N–Me interaction with the cycle. It is clear that for substituents on HN–X bulkier than Me, the cis amide becomes even less stable than the trans (for example in the $CONHC_6H_5$ derivative of [18-6] **7**, the amide bond is trans).

The above results led us to build the ammonium complexes of the CONHMe derivatives with the trans amide only, and starting from the three representative conformers (H_i,H_i), (H_i,O_i), and (O_i,O_i).

Molecular dynamics simulations starting with both (H_i,H_i) and (O_i,O_i) derivatives were carried out by using the charges of SET2. Within the first 10 ps, the metastable (O_i,O_i) conformer converts into (H_i,H_i). For the simulation of the (H_i,H_i) conformer, the rms motion is 0.70 Å for the atoms in the cyclic moiety compared to only 0.45 Å for the corresponding atoms in the C_2 conformation of [18-6]. The motion of the lateral arms is slightly larger (rms motion 1.0 Å) than for the atoms of the cycle.

(2) Conformation of the Lateral Amide Chains in the MeNH$_3^+$ Complex of [18-6](CONHMe)$_2$. The MeNH$_3^+$ complexes of [18-6](CONHMe)$_2$ have been optimized with the two sets of charges on CONHMe in the three characteristic conformations of the lateral chains.

The most important result in Table IV is *a reverse in the relative stabilities upon complexation.* For the free macrocycles the stabilities increase in the order $(O_i,O_i) < (H_i,O_i) < (H_i,H_i)$, whereas for the MeNH$_3^+$ complexes, they increase in the order $(H_i,H_i)^+ < (H_i,O_i)^+ < (O_i,O_i)^+$; ΔE = 0.0, −10.6, and −13.5 kcal/mol with the charges of SET1 and ΔE = 0.0, −11.2, and −22.7 kcal/mol with the charges of SET2.

This reverse in stability can be understood from the energy component analysis summarized in Table IV. The charges of SET2 are more polarized than those of SET1 and thus give larger electrostatic interactions. However, with both sets, it appears that the stability of the complexes is dominated by the interactions between MeNH$_3^+$ and the macrocycle rather than by the energy of the receptor within the complex.

The interaction between NH$_3^+$ and the [18-6] fragment remains close to the −46 kcal/mol in $(H_i,H_i)^+$, $(H_i,O_i)^+$, and $(O_i,O_i)^+$ (respectively, −46.2, −45.9, and −44.8 kcal/mol), and there is no noticeable interaction between CONHMe of the receptor and Me of the substrate. This contrasts with the NH$_3^+$/CONHMe interactions, which are clearly conformation dependent. They are repulsive in $(H_i,H_i)^+$ (9 and 13 kcal/mol with SET1 and SET2), weakly attractive in $(H_i,O_i)^+$ (5 kcal/mol for SET1 and SET2), and strongly attractive in $(O_i,O_i)^+$ (17 and 25 kcal/mol). As a result, compared with unsubstituted [18-6], *the addition of lateral CONHMe chains favors or disfavors the complexation of MeNH$_3^+$, depending on their conformation*: ΔE_c = −3.9 to −8.2 kcal/mol for $(O_i,O_i)^+$, but ΔE_c = +9.7 to +13.9 kcal/mol for $(H_i,H_i)^+$.

As a consequence of the NH$_3^+$/CONHMe interaction, the position of NH$_3^+$ is perturbed by the lateral functionalization of the macrocycle. In $(O_i,O_i)^+$, NH$_3^+$ is attracted by the C=O group, but remains at the center of the cavity, at higher altitude (1.65 Å), with the C–N axis bent. The anchoring results from two NH$^+$···OCH_2 bonds, two NH$^+$···O=C bifurcated bonds, and one NH$^+$···OCH_2 linear bond. The NH$_3^+$/O=C interaction largely compensates for the loss of interaction with the ether oxygens (ΔE = 1.2 kcal/mol only for NH$_3^+$/cycle). The anchoring of MeNH$_3$ in $(H_i,H_i)^+$, where the C=O's are "out", is the same as in the unsubstituted [18-6] with three linear H bonds.

(3) Conformational Change upon Complexation. Since the most stable (H_i,H_i) conformer of the free macrocycle gives the least

stable $(H_i,H_i)^+$ complex, a conformational change of the macrocycle from (H_i,H_i) to (O_i,O_i) has to take place upon the complexation of the cation. In the gas phase, the complexation is probably a downhill process without activation energy. We wanted to model the reorientation of the lateral CONHMe chains when NH_3^+ approaches the anchoring site of the macrocycle, in order to determine if the induced conformational change is "early" or "late".

To do so, as a first test, we placed $MeNH_3^+$ at 4.5 Å above the cycle and rotated smoothly one arm from (H_i,H_i) to (H_i,O_i). We found no barrier for this rotation, in contrast with what is observed in the absence of $MeNH_3^+$ (see Figure 8).

As a second test for this "induced fit" of the receptor, we constrained $MeNH_3^+$ at different altitudes over the (H_i,H_i) and (O_i,O_i) conformers, from 1.5 to 8.5 Å at 1-Å intervals and optimized the energy. We found that above 7.2 Å $(H_i,H_i)^+$ is preferred, whereas below 7.2 Å $(O_i,O_i)^+$ is the more stable. Because the minimizer cannot move the structure over local minima, it is difficult to trace a reaction path for the $(H_i,H_i) \rightarrow (O_i,O_i)$ conversion upon complexation. Our molecular mechanics calculations, however, clearly demonstrate that the conformational changes of the receptor are induced by the approach of the substrate at fairly large distances, and are thus "early".

Molecular dynamics simulations were carried out on $(H_i,H_i)^+$ and $(O_i,O_i)^+$ conformers of the complexes. Within the first 10 ps the $(H_i,H_i)^+$ conformer converts to $(O_i,O_i)^+$. The average rms atomic fluctuations for the cyclic moiety are comparable for $(O_i,O_i)^+$ and for $[18\text{-}6]/MeNH_3^+$ (0.4 Å). Also, the lateral arms are more flexible (rms motion 0.7–0.8 Å) than the ring. It is interesting to find that the lateral arms increase the mobility of the $MeNH_3^+$ substrate in $(O_i,O_i)^+$ compared to $[18\text{-}6]/MeNH_3^+$. The rms motion of the nitrogen (N^+) is 0.95 Å in the former and 0.25 Å in the latter. Also, the average N···O distance is slightly larger (3.4 Å) in the former than in the latter (3.1 Å). This may seem paradoxical in view of the strong interaction energy of $MeNH_3^+$ with $[18\text{-}6](CONHMe)_2$ than with [18-6], but can be understood by the fact that the $MeNH_3^+$ tends to oscillate between the ether oxygens of the anchoring group and the carbonyl oxygens of the lateral substituents.

(4) Role of Lateral Substituents on the Uncomplexed Face of $[18\text{-}6](CONHMe)_2$. To What Extent May They Be Neglected? In our models only the complexed face of the [18-6] cycle bears lateral substituents. This is however a simplified model of the synthetic tetrasubstituted macrocycles with lateral arms on both sides of the cycle.[24,39] One may ask to what extent such a simplification perturbs the central, lateral effects or the conformational change of lateral arms calculated above. A first effect of additional amide substituents may be to rigidify the cyclic moiety and the lateral cavity by formation of the O_{cycle}···HN bonds as seen above in the uncomplexed (H_i,H_i) derivative. A second effect, which we wish to consider here, is to perturb the electrostatic field at the binding sites.

To do so, we started with the $MeNH_3^+$ complex of $[18\text{-}6](CONHMe)_2$ and added two carboxylate substituents COO^- on the uncomplexed face of the receptor (see Figure 1, macrocycle **4**). We used a 1– charge spread over the two carboxylates and optimized the three typical conformers of the amide chains. The results obtained with the charges of SET2 (Table V) clearly demonstrate the attractive effect of these carboxylate groups on $MeNH_3^+$ with the complex, leading to an additional attraction depending on the conformation of the macrocycle (from 17 to 23 kcal/mol).

The important point is that the preferred conformation of the amide fragment still holds qualitatively for the uncomplexed and complexed macrocycles. The order of stability $(H_iH_i) > (H_iO_i) > (O_i,O_i)$ remains (ΔE = 0.0, 5.5, and 14.3 kcal/mol, respectively), but $(O_i,O_i)^+ > (H_i,O_i)^+ > (H_i,H_i)^+$ (ΔE = 0.0, 17.6, and 37.4 kcal/mol).

Concerning the optimized structures it is interesting to note, however, that NH_3^+ anchoring is quite similar in the presence or absence of the carboxylate substituents: despite their attractive effect on NH_3^+, the substrates stay in a "perched position" over the crown, at about the same altitude (see Table V), with the C–N axis slightly bent.

Table V. Energies of the Complex between $^-(CO_2)_2[18\text{-}6](CONHMe)_2$[a] and $MeNH_3^+$. Comparison with the Energies of the Complex $[18\text{-}6](CONHMe)_2/MeNH_3^+$

	CONHMe conformatn[b]		
	$(H_i,H_i)^+$	$(H_i,O_i)^+$	$(O_i,O_i)^+$
E_t[b]	−142.3	−154.4	−165.4
E_c[b]	−55.1	−72.7	−92.5
E_{int}[b]	−55.5	−73.0	−92.5
ΔE_c[c]	0.0	−17.6	−37.4
δE_c[d]	22.9	24.4	38.0
$\Delta E(COO^-)_2$[e]	−124.1	−124.9	−125.4
$E_{rec\ free}$[f]	−87.2	−81.7	−72.9
E_{rec}[g]	−88.1	−82.0	−73.4
h[h]	1.02	1.21	1.45

[a] Receptor **3**. See Figure 1. [b] See Figure 7 and Table IV for the definitions. [c] Complexation energy relative to that of the $(H_i,H_i)^+$ complex. [d] Complexation energy compared to the $(COO^-)_2[18\text{-}6](CONHMe)_2/MeNH_3^+$ complex in the same conformation (charges of SET2). [e] Difference between the optimized energies of $MeNH_3^+$/**3** and $MeNH_3^+/[18\text{-}6](CONHMe)_2$. [f] Optimized energy of the free macrocycle **3**. [g] Energy of the macrocycle **3** within the complex. [h] Altitude (in Å) of nitrogen above the [18-6] fragment mean plane of **3**.

Table VI. Energies[a] and Geometries of $[18\text{-}6](CONHMe)_2/Am^+$ Complexes in the $(O_i,O_i)^+$ Conformation: Site Effect

	ammonium		
	$MeNH_3^+$	$Me_2NH_2^+$	Me_3NH^+
positn of ammonium[b]	C_{3v} or C_2	C_{3v}, C_2, or $C_{3v'}$	$C_{3v'}$ or C_2
positn of ammonium[c]	C_{3v}	C_{2v}	C_{2v}
E_t	−40.9	−33.0	−28.3
E_c	−54.5	−46.2	−41.0
ΔE_c[d]	0.0	8.3	12.5
E_{int}	−69.0	−57.9	−53.6
δE_c[e]	−8.3	−2.5	−2.0

[a] E_t, E_c, and E_{int} are defined in Table II. [b] Before optimization. [c] After optimization, see Figure 4. [d] Complexation energy relative to that of the $(O_i,O_i)^+/MeNH_3^+$ complex. [e] Change in complexation energy brought about by the lateral CONHMe substituents ($\delta E_c = E_c - E_c[18\text{-}6]/Am^+$ complex).

(5) Complexation of $MeNH_3^+$, $Me_2NH_2^+$, and Me_3NH^+ by $[18\text{-}6](CONHMe)_2$: Effect of Lateral CONHMe Substituents on Central Recognition. As in the unsubstituted crown, we compare here the anchoring of primary/secondary/tertiary alkylammonium ions to the macrocycle **2**. Therefore, the complexes with $MeNH_3^+$, $Me_2NH_2^+$, and Me_3NH^+ substrates in various positions [C_{3v}, $C_{3v'}$, or C_{2v} (Figure 4)] have been optimized. Here we have considered the most stable form (O_i,O_i) of the macrocycle and performed the calculations with the more polarized set of charges on CONHMe (SET2, Table IV) in order not to underestimate the interactions within the complexes.

The results of Table VI show first that lateral substituents stabilize all the complexes, but not to the same extent: $MeNH_3^+$ is more stabilized than $Me_2NH_2^+$ or Me_3NH^+. As a result, *the binding selectivity for primary ammonium, compared to secondary and tertiary substrates, is increased upon addition of lateral amide substituents*: ΔE = 0.0, 8.0, and 13.5 kcal/mol; compared with 0.0, 2.4, and 7.0 kcal/mol for the unsubstituted [18-6]. This lateral discrimination results mainly from steric hindrance caused by CONHMe, which may lead to a repositioning of the substrate. For example, Me_3NH^+ cannot remain in the $C_{3v'}$ position over the cycle, but becomes C_{2v} (ΔE = 2.3 kcal/mol between these two forms). Whereas the notion of central recognition has been introduced to distinguish between the anchoring of primary, secondary, and tertiary ammonium ions,[1,23,24] we show that this effect cannot be considered separately from the lateral recognition, even for bulkier substituents.

(6) Complexation of RNH_3^+ by $[18\text{-}6](CONHMe)_2$ as a Function of R: Effect of Lateral Arms on Lateral Recognition.

Table VII. Vicinal Effect in [18-6](CONHMe)$_2$/Ammonium Complexes[a]

ammonium	E_t	E_c	ΔE_c[b]	δE_c[c]	E_{int}	Δh[d]
$MeNH_3^+$	−40.9	−54.5	0.0	−8.2	−69.0	0.0
$EtNH_3^+$	−40.5	−54.9	−0.4	−8.7	−68.8	0.1
$C_6H_5NH_3^+$	−43.5	−59.0	−4.5	−8.7	−73.8	0.89
$^+$Gly-OMe	−56.7	−60.0	−5.5	−9.7	−73.7	0.79
$^+$Gly(Phe)-OMe	−51.4	−62.4	−7.9	−7.1	−74.6	0.95
$^+$Gly-Gly-OMe	−55.2	−58.2	−3.7		−69.3	0.81
$^+$Gly-Phe-OMe	−46.5	−58.5	−4.0		−72.0	0.84

[a] E_t, E_c, and E_{int} are defined in Table II. [b] Complexation energy relative to that of the $(O_i,O_i)^+/MeNH_3^+$ complex. [c] Change in complexation energy brought about by the lateral CONHMe substituents ($\delta E_c = E_c - E_c$[18-6]/$MeNH_3^+$ complex). [d] Variation of the altitude of nitrogen above the [18-6] cycle for RNH_3^+ compared to $MeNH_3^+$.

Table VIII. Energies of $^+$Pro-OMe and $Me_2NH_2^+$ Complexes with [18-6] and [18-6](CONHMe)$_2$[a]

receptor	[18-6]	[18-6](CONHMe)$_2$
$^+$Pro-OMe		
E_t	28.4	−17.7
E_c	−45.2	−51.6
E_{int}	−49.1	−62.7
$E_{B/S}$[b]		−26.4
$Me_2NH_2^+$		
E_t	12.3	−33.0
E_c	−43.7	−46.2
E_{int}	−45.0	−57.9
$E_{B/S}$[b]		−22.5

[a] E_t, E_c, and E_{int} are defined in Table II. [b] Interaction energy between the lateral branches CONHMe and the substrate.

We now consider the complexes between the most stable conformer (O_i,O_i) of **2** and the various organic substrates anchored by a primary ammonium site ($MeNH_3^+$, $EtNH_3^+$, $C_6H_5CH_2NH_3^+$, $^+$Gly-OMe, $^+$Gly(Phe)-OMe, $^+$Gly-Gly-OMe and $^+$Gly-Phe-OMe) in order to assess the effect of lateral interaction between R of the substrate and the CONHMe arm of the receptor on binding affinity and selectivity.

The results reported in Table VII, obtained with the charges of SET2, show that *lateral substituents enhance the complexation energy E_c in all cases* (by 7–10 kcal/mol). The range, as a function of R (~3 kcal/mol), is small compared to the range calculated for the primary site effect (12 kcal/mol) because in these R-NH_3^+ complexes, the strongest interaction between NH_3^+ and the [18-6] cycle or CONHMe remains comparable in all complexes. It may be, however, perturbed by a repositioning of the substrate in the cavity of the receptor. Compared with $MeNH_3^+$, the NH_3^+/cycle interaction decreases by 2.2, 3.0, 3.2, 3.3, and 4.4 kcal/mol, respectively, in $^+$Gly(Phe)-OMe, $^+$Gly-Gly-OMe, $^+$Gly-OMe, $^+$Gly-Phe-OMe, and $C_6H_5CH_2NH_3^+$. This is compensated for by the NH_3^+/CONHMe interactions, stronger with $C_6H_5CH_2NH_3^+$ and $^+$Gly-OMe (−25.9 and −23.8 kcal/mol) than with $EtNH_3^+$, $MeNH_3^+$, the dipeptides (−23.4, −22.5, −22.4, and −22.3 kcal/mol), or $^+$Gly(Phe)-OMe (−18.1 kcal/mol). In these ammonium complexes of lateral CONHMe derivatives, NH_3^+ tends to move "up", toward the C=O groups, and the altitude of N increases (see Table VII). The $NH^+\cdots O{=}C$ distances range from 2.20 to 2.65 Å.

With R = Me, Et, $C_6H_5CH_2$, and $MeOOCCH_2$, the C–NH_3^+ bond axis is bent over the cycle, with R equidistant from the two carbonyls. This is in contrast with the "perpendicular" position calculated in the $MeNH_3^+$ complex of the unsubstituted [18-6] and clearly results from substituent effects. For $^+$Gly(Phe)-OMe, however, we find the C–N axis perpendicular.

Turning now to the analysis of the stability of the RNH_3^+ complexes of [18-6](CONHMe)$_2$ as a function of R (Table VII), we find an increased complexation energy compared with $MeNH_3^+$ or $EtNH_3^+$ (4–8 kcal/mol). The CONHMe/R interactions are attractive, mainly of the Van der Waals type with $C_6H_5CH_2NH_3^+$, and electrostatic with the amino acids and dipeptides.

No significant stabilization (i.e., less than 1 kcal/mol) is found when the size of R is increased from amino acids to dipeptides. This is because the second amino acid interacts very weakly with CONHMe, and its amide part (CONH), α to C–NH_3^+ contributes negatively to the stability. As a result, the macrocycle **2** should be unable to select between amino acid and dipeptide substrates.

(7) The Complex of Proline Methyl Ester. We have performed calculations on the complex between [18-6](CONHMe)$_2$ and proline methyl ester ($^+$Pro-OMe) in order to compare its stability with that of $Me_2NH_2^+$ and thus to analyze more specifically the lateral recognition of a N-substituted substrate. The results are reported in Table VIII.

Compared with $Me_2NH_2^+$/**2**, the complex $^+$Pro-OMe/**2** is stronger (ΔE_c = 5 kcal/mol), but is still weaker than the complexes with primary ammonium ions.

The gain of stability arises first from a better anchoring to the [18-6] fragment. In fact, in the complexes with unsubstituted [18-6], we calculate a greater stability for $^+$Pro-OMe than for $Me_2NH_2^+$ (E_c = −45.2 and −43.7 kcal/mol, respectively) resulting from vicinal interactions between the ester group of $^+$Pro-OMe and the cycle.

Additional stabilization is due to the lateral CONHMe arms, which interact better with $^+$Pro-OMe than with $Me_2NH_2^+$ (−6.4 and −2.5 kcal/mol, respectively).

As a result of these two effects, the disubstituted macrocycle **2** should discriminate between secondary ammonium substrates.

(8) Enhanced Lateral Recognition by Incremental Addition of Lateral Chains: Dicysteinyl Derivative 4 and Its RNH_3^+ Complexes. Because the CO-Cys-OMe tetraderivative **5** reacts faster with $^+$Gly-Phe-OMe than with $^+$Gly-OMe, we decided to model the dicysteinyl derivative **4** complexed with various RNH_3^+ substrates. The comparison with [18-6](CONHMe)$_2$ will give insight into the effect of increasing the length of lateral chain on binding affinity and selectivity for amino acids ($^+$Gly-OMe, $^+$Gly(Phe)-OMe) versus dipeptides ($^+$Gly-Gly-OMe, $^+$Gly-Phe-OMe).

For the free receptor and the complexes, many conformations for the lateral chains are possible, and a sampling of the conformational space would be very time consuming. In view of the above results and of our goal to model the intracomplex thiolysis reaction, we started from the (O_i,O_i) conformation of the lateral arms and positioned graphically the OMe and SH groups of these arms in such a way that the lone pairs of SH are directed inside the cavity toward the substrate.

After optimization, we find that compared with [18-6](CONHMe)$_2$, the lengthening of lateral substituents increases the stability of the four complexes (ΔE = 1.2, 2.1, 3.6, and 4.3 kcal/mol, respectively, for $^+$Gly-OMe, $^+$Gly(Phe)-OMe, $^+$Gly-Gly-OMe, and $^+$Gly-Phe-OMe).

The energy analysis shows that the anchoring of the substrates is very similar to that found in the [18-6](CONHMe)$_2$ complexes. In particular, the NH_3^+/B interaction (from −23 to −25 kcal/mol) and the NH_3^+/cycle interaction (from −44 to −45 kcal/mol) remain comparable.

The second interesting result is the differential binding affinity of amino acids compared to dipeptides by the dicysteinyl derivative of [18-6]. The complexes with $^+$Gly-Gly-OMe and $^+$Gly-Phe-OMe are more stable than with $^+$Gly-OMe and $^+$Gly(Phe)-OMe (from 3 to 5 kcal/mol) because of the better receptor/substrate interaction for the dipeptide substrates.

In the optimized complexes and the distance between the reactive groups COOMe of the substrate and the SH of the receptor is much shorter with the dipeptides (less than 3 Å) than with the amino acids (more than 5 Å). In the latter, we checked graphically that a translation of ~3 Å is necessary in order to bring the ester and thiol groups in close enough proximity for reaction to occur. According to Figure 6, this would cost ~8 kcal/mol, which would, in practice, slow the intracomplex reaction. We thus show that two effects favor the thiolysis of dipeptides versus amino acid substrates: a better binding and a better positioning of the reactive groups.

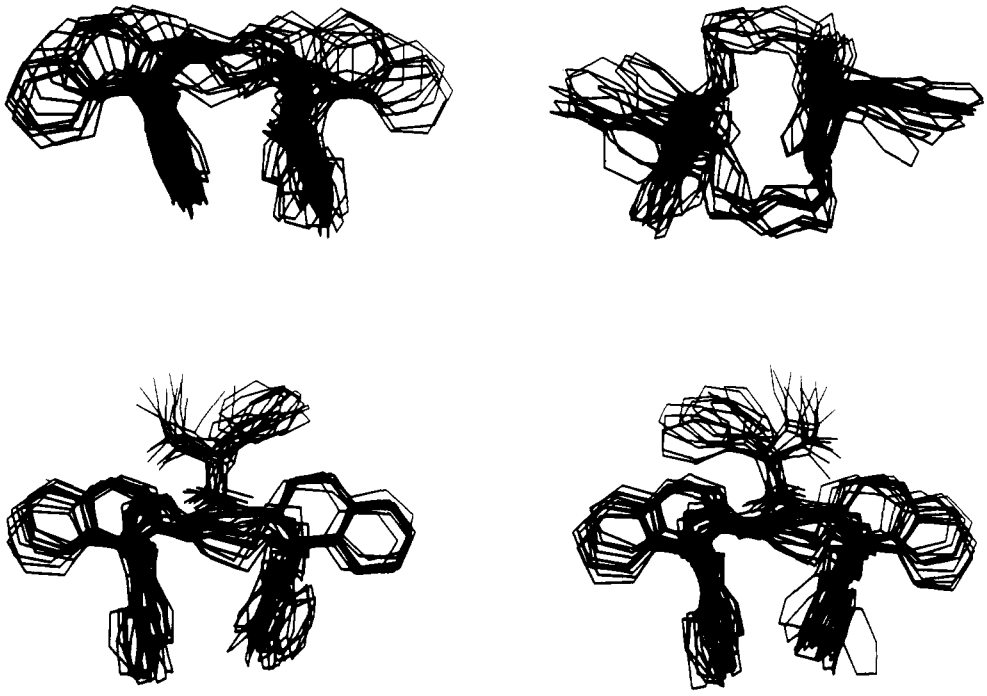

Figure 9. Dynamics structures for the free macrocycle **9a** (above) and for its L complex with phenylglycine methyl ester (below). Top: uncomplexed, looking parallel (left) and perpendicular (right) to the ring plane. Bottom: the D (left) and L (right) complexes of $^{+}$Gly(Phe)OMe. Note the reduced motion of the receptor upon complexation.

(C) **Enantiomeric Recognition upon Complexation.** The discrimination between enantiomeric substrates by a chiral macrocyclic receptor is weak, and small energy differences (in the range of 1 kcal/mol) are involved. This contrasts with the high stereoselectivity of enzyme catalysis, probably because in that case, the selectivity is due to transition-state effects rather than initial binding effects.[10] We wanted however to address computationally the problem of stereoselectivity at the step of complexation. We thus felt it important to test first the capability of our computational method and force field to account for the L/D selectivity displayed by the Cram's macrocycle **9a** (Figure 3) and then to assess whether the lateral substituted derivatives of [18-6] are potential candidates for the chiral recognition of ammonium substrates.

(1) Complex between the Methyl Ester of Phenylglycine and the Cram Macrocycle 9a. We started with several positions of the L and D substrates in the complex and found that, in the most stable optimized structure (L), the phenyl and ester substituents are between the naphthyl "walls" of the receptor. The other five conformations are higher in energy. Such a disposition is also observed in the X-ray structure of the complex with **9b** and the D substrate (Figure 3). For comparison, the uncomplexed **9a** has also been optimized in the same conditions.

We calculated complexation energies of −58.5 and of −57.2 kcal/mol for the lowest energy L and D substrates, respectively. These values are larger than E_c calculated for the same substrate complexed by unsubstituted [18-6] (by 3.2 and 1.9 kcal/mol, respectively) as a result of attractive van der Waals interactions between the naphthyl walls of the receptor and R of the substrate. E_c is smaller than in the corresponding complexes with [18-6]-$(CONHMe)_2$ (**2**; ΔE_c = 3.9 and 5.2 kcal/mol, respectively).

It is satisfying to find that the L complex is more stable than the D (by 1.3 kcal/mol), in qualitative agreement with the experimental difference of the association free energies measured in $CHCl_3$ ($\Delta\Delta G$ = 2 kcal/mol[26]). We thus account with a simple molecular mechanics approach for the enantioselectivity of complexation in the Cram system. It results from steric rather than electrostatic factors. In fact, energy component analysis shows that the receptor/substrate electrostatic interactions are comparable for the L and D complexes, whereas the van der Waals energy component is more attractive in the L than in the D complex. This results from a more favorable position of the substrate between the naphthyl walls in the L complex; in particular, the phenyl group of the cation tends to adopt a stacking position with a naphthyl of the macrocycle.

Our analysis suggests that the L/D recognition in this system should not depend much on the dielectric constant of the medium. In order to test that point computationally, we have reoptimized the L and D complexes with a dielectric constant equal to 10 instead of 1, and we found that the relative stabilities of L/D complexes remain comparable (ΔE(L/D) = 1.6 kcal/mol).

It is also interesting to compare the energy of the receptor within the complex to its energy optimized in the absence of substrate. We find a difference of 4 kcal/mol, which corresponds to the strain induced upon anchoring of the ammonium substrate. This is quite small compared with the energy gained upon complexation (~50 kcal/mol). Examination of both structures on the graphic display clearly shows that, upon relaxation, the polyether ring of the free receptor becomes more planar and the naphthyl groups adopt an unsymmetrical disposition with respect to that plane: the two above tend to move slightly away from each other, whereas the two below tend to stack.

Molecular dynamics simulations on Cram's macrocycle free and complexed with L and D $^{+}$Gly(Phe)-OMe were carried out. Figure 9 displays views of the dynamics structures for the free macrocycle and for the L complex.

For the free host, relatively large amplitude motions are observed, with the cycle having an average rms motion of 0.9 Å. The naphthyl groups display interesting dynamic behavior, in that the two on the "open" face have larger motion (1.3 Å) than those on the "closed" face (0.9 Å). Upon complexation with either L or D substrates, there is significant rigidification of all these structural components, with rms values of 0.4–0.5 Å for the cycle, 0.6–0.8 Å for the open face, and 0.5–0.8 Å for the closed face. Thus, complexation makes the two faces behave more equivalently in their dynamic motion.

For the substrate, the dynamic behavior of the NH_3^+ group is similar to that found in [18-6]/$MeNH_3^+$, with average N···O distance of 3.1 Å and rms fluctuations of the nitrogen position of 0.4 Å. However, the nonanchored part of the substrate displays higher mobility, with the phenyl group having rms motion of 1.3 (L) to 1.1 (D) Å and the COOMe having rms motion of 0.9 (L)

Table IX. Energies[a] of Optimized L/D Diastereoisomeric [18-6](CONHMe)$_2$/$^+$Gly(Phe)-OMe Complexes

	CONHMe conformatn					
	$(H_i,H_i)^+$		$(H_i,O_i)^+$		$(O_i,O_i)^+$	
	L[c]	D[c]	L[c]	D[c]	L[c]	D[c]
E_t	−33.9	−34.9	−42.5	−44.2	−51.5	−51.4
E_c	−44.9	−45.9	−53.5	−55.2	−62.5	−62.4
ΔE(L/D)[b]	1.0	0.0	1.7	0.0	−0.1	0.0
E_{int}	−46.3	−46.2	−59.2	−62.3	−75.2	−74.6

[a] E_t, E_c, and E_{int} are defined in Table II. [b] ΔE(L/D) = E_t(L) − E_t(D). [c] $^+$Gly(Phe)-OMe enantiomer.

to 1.3 (D) Å.

For the D complex, one can compare the average position of the atoms over the 50-ps simulation to the positions in the X-ray structure. The rms found (0.45 Å) is larger than the rms between the energy minimized and experimental static structures (0.06 Å), but remains small.

(2) Can the [18-6](CONHMe)$_2$ Chiral Macrocycle Display Chiral Recognition? We have considered the complexes formed with two chiral substrates: first, the methyl ester of phenylglycine, because we have seen that this highly unsymmetrical ammonium ion led to a high recognition by the Cram's macrocycle; second, the dipeptide $^+$Gly-Phe-OMe (with a chiral center in a remote position from the anchoring site), because its thiolysis by the tetracysteinyl derivative **5** is stereoselective.[25]

For the complexes with $^+$Gly(Phe)-OMe we have considered the (H_i,H_i), (H_i,O_i), and (O_i,O_i) conformers of the crown (Table IX), and we have found that the most stable L and D complexes are $(O_i,O_i)^+$. For this symmetrical conformation of the receptor, however, no noticeable L/D difference is calculated (ΔE(L/D) = 0.1 kcal/mol). Interestingly, the largest chiral recognition is obtained with the unsymmetrical conformer $(H_i,O_i)^+$, where the D substrate is perferred over the L by 1.7 kcal/mol. The difference comes mainly from electrostatic interactions between R of phenylglycine methyl ester and the CONHMe lateral substituents, which is more favorable with the D substrate.

For dipeptides, only the $(H_i,O_i)^+$ complex with $^+$Gly-Phe-OMe has been considered because we have seen that the dissymetrical conformation of the macrocycle leads to the largest stereoselectivity. Due to the potential interactions between the lateral CONHMe and Phe-OMe of the dipeptide, L/D differentiation was expected; however, we find only a small preference for the L substrate (0.6 kcal/mol).

Discussion

Choice of the Computational Method and the Force Field. A molecular mechanics approach, which includes both intra- and intermolecular energy components, has been used to calculate the total energy of supermolecules formed by the association of ammonium substrates and [18-6] derivatives.

Our approach was first to calibrate a simple model to account for experimental gas-phase enthalpies for ammonium/crown ether complexes. This has led to results in better agreement with experiment than those from small basis set ab initio calculations. For example, ab initio calculations at the STO3G level on the NH_4^+/OMe_2 complex[52] afford a complexation energy of −38.5 kcal/mol, which is approximately 16 kcal/mol more than the observed value in the gas phase for the $MeNH_3^+/OMe_2$ complex.[22]

Likewise, we preferred to calibrate the interaction between $MeNH_3^+$ and [18-6] with this simple model rather than with a more elaborate representation calibrated with NH_3^+/monoether interactions. For comparison, we calculated the complexation energy of the $MeNH_3^+$/[18-6] complex using the force field of Claverie et al.[53] These authors used a 6-exp potential rather than a 6–12, and they included polarization in addition to a coulombic term to represent the electrostatic interaction. With our calibrated charges on NH_3^+, we calculated E_c values of −89 and −83.5 kcal/mol, respectively, for the "C_2" and "D_{3d}" complexes. Although Claverie's force field is more rigorous since it includes polarization, in its present form it clearly overestimates the interaction energy.

It seems to us that an adequate calibration of the electrostatic component based on available experimental data is essential prior to adding other effects. Also, one needs to recalibrate the electrostatic parts in a force field in which polarization is included.

Our approach is essentially "gas phase", and we do not include solvent either explicitly or implicitly via the dielectric constant. Thus, the absolute or relative complexation energies should not be directly compared with the experimental values in solution, as the solvent has a large leveling effect.

For example, the difference of relative binding affinity for $MeNH_3^+$ and Me_3NH^+ complexed by [18-6] is $\Delta\Delta H$ = 5 kcal/mol in the gas phase,[22] whereas in water this difference is only 0.6 kcal/mol.[24] In addition, the absolute binding affinity is larger in the gas phase (−46 kcal/mol[22]) than in water (−1.5 kcal/mol).[24] Our simple model does not include entropic effects, relative solvation energies, which are clearly required to reproduce the relative complexation energies in solution.

However, our calculations account for a number of the trends in the central, lateral, and enantiomeric effects on molecular recognition that have been observed in solution.[23]

Central Discrimination of Primary, Secondary, and Tertiary Ammonium by [18-6]. The calculations clearly show that the [18-6]/ammonium complex stability is strongly dependent on the cation binding mode (see Figure 4) and on the number of $NH^+\cdots OCH_2$ interactions that tend to be linear. However, our results, and the gas-phase data, show that the corresponding energy is not proportional to the number of hydrogen bonds. For instance, the energy loss is only 12% from $MeNH_3^+$/[18-6] to Me_3NH^+/[18-6]. This remark corroborates ab initio STO3G calculations of the interaction energy between HF and NH_4^+, $MeNH_3^+$, $Me_2NH_2^+$, and Me_3NH^+ (18.1, 16.5, 15.5, and 14.8 kcal/mol).[54] This is because the interaction remains electrostatic, with a total charge of 1+ on the ammonium.

Depending on the nature of the ammonium ion, a particular binding mode to [18-6] has been observed for each cation. We find, in agreement with X-ray studies, that the "D_{3d}" conformation of [18-6] is slightly preferred for complexes with primary ammonium ions.[27-29] On the other hand, the "C_2" complex has a comparable energy and is likely to be observable in the gas phase. Interestingly, the "C_2" conformer is clearly favored in the secondary ammonium complex. Thus, an optimal complementarity is obtained between partners having similar symmetries.[55]

Our calculations point out that the flexibility of the [18-6]/RNH_3^+ supermolecule with respect to the conformation of the cycle itself and the anchoring of NH_3^+. In agreement with previous experimental or theoretical studies,[15,34,44,45] we suggest that conformers other than "D_{3d}" or "C_2", not characterized by X-ray, might be present in the gas phase or in solution.

Mobility of the Cation Anchoring to [18-6]. In the optimized structur of the [18-6]/$MeNH_3^+$ complex, the ammonium is anchored by $NH\cdots OCH_2$ linear hydrogen bonds and rests in a perched position above the macrocycle. Such a situation has also been observed in the X-ray structure of NH_4^+,[27] $MeNH_3^+$,[28] and $C_6H_5CH_2NH_3^+$[30] complexes of [18-6]. Ab initio calculations have also pointed out the tendency for linear rather than nonlinear hydrogen bonds in proton donor/acceptor complexes.[56-58] However, the ammonium may be displaced from its equilibrium position, move, bend, or turn around the C–N bond axis as ob-

(52) Timko, J. M.; Moore, S. S.; Walba, D. M.; Hiberty, P. C.; Cram, D. J. *J. Am. Chem. Soc.* **1977**, *99*, 4207–4219.
(53) Gresh, N.; Claverie, P.; Pullman, A. *Theor. Chim. Acta* **1984**, *66*, 1.
(54) Flaker, H. T.; Boyd, R. J. *Can. J. Chem.* **1985**, *63*, 1562–1567.
(55) Mislow, K. *Bull. Soc. Chim. Belg.* **1977**, *86*, 595–601.
(56) A perching position of NH_3^+ favors linear $NH_+\cdots OCH_2$ interactions. This preference for linear hydrogen bonds over bifurcated ones has also been calculated at the STO 3G level by Pullman et al. in the complex of NH_4^+ with nonactin[57] and OH_2[58] and by Flaker and Boyd in the complex $MeNH_3^+\cdots FH$.[54]
(57) Gresh, N.; Pullman, A. *Int. J. Quantum Chem.* **1982**, *22*, 709–716.
(58) Pullman, A.; Berthod, H.; Gresh, N. *Int. J. Quantum Chem.* **1976**, *10*, 59–76.

served in the molecular dynamics simulations.

The corresponding rotational barrier that we have calculated with our simple electrostatic model is, however, a lower bound, because charge transfer and polarization energies are stronger in a linear arrangement and favor the optimized structure in which NH^+ bonds point toward the oxygen atoms of the "D_{3d}" cycle.

We disagree with the conclusion of Yamabe et al., who calculated by a CNDO method[16] that it requires 8 kcal/mol (10 times our value) to move NH_4^+ 0.5 Å from of its equilibrium altitude above the [18-6] cycle. Part of the difference between our results and those of Yamabe may be due to the fact that CNDO/2 overestimates the charge-transfer energy with respect to the electrostatic, thus favoring strong interactions within short distances. To our knowledge, the gas-phase complexation energy of the NH_4^+/[18-6] has not been determined, but should remain comparable or slightly superior to that of the $MeNH_3^+$/[18-6] complex (−46 kcal/mol). Thus, Yamabe's calculations overestimate this energy (−86 kcal/mol[16]).

There is experimental evidence relating to the mobility of the cation anchored in the cavity of [18-6]. The complexes between [18-6] and $MeNH_3^+$, $HONH_3^+$, and $H_2NNH_3^+$ have been found to be of comparable strength in methanol;[23] however, their X-ray structures[28] show that NH_3^+ is anchored above the macrocycle at various heights ranging from 0.84 to 0.68 and to 0.11 Å, respectively. This variation may arise from electronic perturbations of NH_3^+ by R, and from counterion effects in the crystal.

All these results show that the anchoring of the ammonium substrate to [18-6], although strong, allows some mobility of Am^+. This may be important in order to facilitate an appropriate positioning of the substrate and receptor reactive end groups during the thiolysis reaction performed by the macrocyclic receptor of Figure 2.

Vicinal Effect in the Complexes between [18-6] and RNH_3^+. When the RNH_3^+ cations bear alkyl and/or ester substituents, the anchoring of the substrate is perturbed, and this leads to an increased stability compared with $MeNH_3^+$. This stabilization arises mainly from attractive van der Waals interactions, which are additive when several vicinal substituents are present, as in the methyl ester of phenylglycine.

These results in "the gas phase" are not surprising since no competition effects (such as solvation or ion pairing) could interfere. They contrast, however, with the experimental data in methanol where the [18-6] crown complexes $MeNH_3^+$, $EtNH_3^+$, and $EtOOCCH_2NH_3^+$ without any pronounced selectivity ($\Delta\Delta G$ = 0, 0.01, and 0.6 kcal/mol[23]). It is very likely that in solution the supermolecules are less compact than in the gas phase, with a weaker anchoring of the ammonium substrate. Such a situation decreases the van der Waals interactions found in our "gas-phase" model.

Lateral Recognition of Ammonium Substrates by the $(B')_2$-[18-6]$(B)_2$ derivatives of [18-6]. The lateral functionalization of [18-6] by CONHMe first acts on the central recognition by increasing the selectivity of complexation of primary ammonium ions versus secondary and tertiary ammonium ions. The lateral arms also increase the receptor/substrate interactions, which leads to a better discrimination of the substrates. In particular, the affinity of the receptor toward primary ammonium bearing polar groups (the amino acid esters) is enhanced. Likewise the lateral CONHMe arms enhance the recognition of $^+$Pro-OMe with respect to $Me_2NH_2^+$.

These trends are the same, but weaker, in aqueous solution with the tetracarboxylate derivative **6** showing a greater selectivity of complexation for $MeNH_3^+/Me_3NH^+$ than unsubstituted [18-6] ($\Delta\Delta G$ = 3 and 1 kcal/mol[24]). Concerning the lateral recognition of primary ammonium ions, **6** binds amino acid esters more strongly than $EtNH_3^+$ ($\Delta\Delta G$ = 1 kcal/mol[24]) and also enables a discrimination between secondary and primary ammonium ions (adrenaline gives a stronger complex than ephedrin, $\Delta\Delta G$ = 0.6 kcal/mol[24]).

Lateral recognition may extend beyond amino acid esters to dipeptides. With [18-6](CONHMe)$_2$, we find no selectivity between these two species. However, lengthening of the lateral arms *B* from *B* = CONHMe (macrocycle **2**) to *B* = CO-Cys-OMe (macrocycle **4**) leads to a preference for the dipeptide ester complexes.

In line with these results, a selectivity has also been found in solution in favor of substrates whose lengths are complementary to those of the [18-6] lateral arms.[24] Such a discrimination, which comes from chain-length complementarity, has also been reported in cylindrical ammonium macrotricyclic cryptates.[59]

Lateral Chain Conformation and Substrate Anchoring to Derivative 2. The binding of ammonium substrates to substituted [18-6] derivatives induces a conformational change in the CONHMe lateral side arms. In the most stable conformation with ammonium substrates, we have shown that anchoring of NH_3^+ comes from the interactions with the cycle and with the two lateral C=O groups. As a consequence, NH^+ tends to point toward these groups, so that the cation is bent above the macrocycle cavity. This induced fit of the macrocycle upon complexation of the ammonium ion may be of great importance in a more general way for the design of a receptor for a given substrate (or vice versa): the use of a rigid receptor or of a single seemingly related X-ray structure may be very misleading.

In solution, one may expect a different solvation effect depending on the outward or inward orientation of the lateral CONHMe chains. This will be interesting to model by simulation techniques.

These results lead us to reconsider the X-ray structure of **7** with Sr^{2+} in its cavity where the NH's of the side arms are "in" rather than the C=O's. In spite of the attraction of Sr^{2+}, the C=O's point outward from the cavity and do not participate in the complexation. Rather than being due to an intrinsic conformational preference, this difference may arise from the particular position of Cl^- coordinated to Sr^{2+}. The anion being between the arms prevents an "in" orientation of the C=O groups.[30]

Finally, typical "in" C=O groups have been observed in the X-ray structure of the complex between **8** (see Figure 1; *B* = *B'* = $CONMe_2$) and KBr.[32] In this crystal, there are two distinct K^+ binding sites. One K^+ is located inside the macrocycle, as in the structure of [18-6]/KBr[27], but the second K^+ rests in a perched position 2.85 Å above the oxygen mean plane at 2.65 Å from the oxygen atoms of the C=O.

It is noteworthy that in solution this complex is slightly more stable than the complex with four lateral CONHMe chains ($\Delta\Delta G$ = 0.6 kcal/mol in water[24]). This is presumably related to the fact that with *B* = CONHMe, complexation requires a conformational change from (H_i,H_i) to (O_i,O_i). For *B* = $CONMe_2$ no such loss of internal H bonding accompanies complexation.

In fact, it is a challenge to design a receptor that would be rigid enough to permit an adequate positioning of both the reactive groups and binding sites and that should be flexible as well to give high structural complementarity with the bound substrate in the noncovalent complex and in the covalent tetrahedral intermediates of the reaction. In this respect there is a difference between these macrocyclic systems and some enzymes such as the serine proteases. Whereas in α-chymotrypsin the active site may be considered as a fairly rigid pocket (confirmed by X-ray comparison of the free enzyme and the tosylated complex[10]), the whole macrocycle is very flexible. In particular, in [18-6] with the lateral arms, some conformations may not have an appropriate cavity of the correct shape for complexation.

In the context of the design of artificial enzymes, the results from our molecular dynamics simulations on $(O_i,O_i)^+$ complexes are of particular interest. In this system, the NH_3^+ group is attracted to both ether and carbonyl oxygen binding sites. This leads both to increased stability of the complexes and mobility of the substrate within the "receptor". In multistep reactions, the use of this mobility may be of critical importance in efficient catalysis.

(59) Lehn, J. M. In *Biomimetic Chemistry*; Yoshida, Z. I., Ise, N., Eds., Elsevier: New York, 1983; pp 163–187. Kotzyba-Hibert, F.; Lehn, J. M.; Vierling, P. *Tetrahedron Lett.* **1980**, 941. Kotzyba-Hibert, F.; Lehn, J. M.; Aigo, K. *J. Am. Chem. Soc.* **1981**, *103*, 4266.

Simplification of the Model. A molecular model is always a simplification of an actual molecule, and one may ask to what extent this model may be simplified. For example, what is the influence of neighboring groups, not directly involved in the substrate anchoring or the thiolysis reaction, upon the above calculated effects? This problem is often met in enyzme modeling when only the active site is considered in order to reduce the computational time.[60] In this respect, our calculations of the COO^- effects, which are also present in enzymes, are of particular interest.

A first effect of the COO^- arms attached to the uncomplexed face of **2** may be structural i.e., it could rigidify the receptor. The quaternary structure of an enzyme acts in the same way as it determines the structure of the active sites. The second effect is electrostatic.

We have shown that **3** (B = CONHMe, B' = COO^-) keeps the same conformational preferences as **2**, complexed or uncomplexed. Its cavity stays cylindrical, thus permitting the inclusion of the substrate.

The carboxylates on the uncomplexed face of the macrocycle increase the stability of the complexes from 18 to 23 kcal/mol (see Table V). Such effect has also been experimentally observed in solution with the tetracarboxylate derivative **6** whose ammonium complexes are significantly more stable than those formed with lateral amide branches or carboxylic derivatives.[24]

However, from a structural point of view, the $MeNH_3^+$ anchoring is not significantly modified. In particular, the altitude of NH_3^+ above the macrocycle is comparable with or without COO^- substituents. This suggests that other effects (e.g., steric or torsional) prevent the NH_3^+ from approaching more closely to the COO^- once the NH_3^+ has been anchored in the cavity. We note that, with B' = COO^-, the global minimum for our gas-phase model might be a $NH_3^+\cdots{}^-OOC$ structure, but this would be a simple artifact of not including solvation effects.

Enantiomeric Differentiation of Ammonium Substrates upon Complexation. Our simple molecular mechanics approach enabled us to reproduce the small energy differences between diastereoisomeric complexes observed in chloroform by Cram et al.,[26] but we were unable to find a simple correlation between these energies and dynamic parameters for these complexes. In addition, we emphasize that only a limited search was made for the optimal L and D structures. Enantiomeric recognition is reasonably easy with a rigid and highly asymmetrical receptor such as the macrocycle **9a** which also develops a greater geometric complementarity with the L enantiomer of phenylglycine methyl ester than with the D. Concerning the complexing power of this macrocycle, experimental data show, in contrast to the results from our calculations, the tendency of the substituted macrocycle **9a** to form less stable complexes than unsubstituted [18-6] crown **1**. We emaphasize, however, that Cram et al. have determined the complexing capability of macrocycle **9a** by a two-phase technique, and the extraction constants may not be directly compared to the stability constants determined by calorimetry[23] and pHmetry,[24] or to our relative complexation energies calculated in the "gas phase", where solvation effects are not included.

With the more flexible derivatives [18-6]$(B)_2$ we show that the L/D difference is very weak and only appreciable for the asymmetric conformers of the macrocycle. An interesting point concerns the effect of the conformation of **2** on enantiomeric recognition. As the CONHMe arms are flexible, the most stable complex $(O_i,O_i)^+$ should form, and we calculate no enantiomeric differentiation with this conformer. However, our calculations suggest that an enhancement of the L/D difference could be obtained in such systems by blocking a metastable dissymetrical conformer [for example, (H_i,O_i)].

It is difficult to come to firm conclusions on the L/D preference when the complexity and the flexibility of the receptor or the substrate increase. This is due to the multiple minima problem and the inherently small L/D energy difference. For example, with macrocycle **4** (B = CO-Cyl-OMe, B' = H), we find a weak preference for the L enantiomer of $^+$Pro-Gly-OMe over the D [ΔE(L/D) = 0.2 kcal/mol], while the difference is in favor of the D enantiomer for $^+$Gly-Phe-OMe [ΔE(L/D) = 0.1 kcal/mol].

A more extensive molecular dynamics study of these complexes may lead to further insights into the multiple minima problem and might permit the comparison of the relative positioning of the L/D reactant groups, which is a typical dynamic process. On the other hand, it is not established whether any L/D recognition takes place in the initial noncovalent complexation step of the receptor and the substrate (studied here); all enantiomeric selectivity may take place in the transition states of the catalyzed reactions, as observed in the stereoselective hydrolysis of peptides and esters.[10,25]

Conclusion

We have presented molecular mechanics calculations on ammonium/ether complexes, which are the basic elements of supermolecules possessing the properties of artificial enzymes.[1-5,7]

A simple model, essentially electrostatic, has been used to represent the interactions within the complexes. In particular, we propose a set of atomic charges on ammonium ion that can be used for various ammonium cations complexed by a [18-6] binding site. Such a set of charges permitted us to model various complexes and to analyze the intermolecular interactions that lead to central, lateral, and vicinal discrimination of these cations. Furthermore, we are able to define "important" structural features such as the conformation of the free or complexed receptor and to characterize a number of interesting differences between dynamic behavior of various of these receptors and their cation complexes.

We also account for the weak energy differences between diastereoisomeric complexes of the Cram macrocycle for which the L/D preference has been found to come mainly from van der Waals interactions. For the lateral derivatives of [18-6] it is difficult to conclude from a limited number of static models when both the receptor and substrates are more flexible and when no steric effects hinder the anchoring of the ammonium. The calculated L/D energy differences are very small.

The general agreement with much of the available experimental and theoretical data validates our simple molecular mechanics/dynamics representation of the receptor/substrate interactions. We have shown that this rather simple model, when adequately calibrated, can be used for medium-size supermolecules.

We can now extend the study of molecular recognition at the simple complexation level by considering explicitly the dynamic aspects of these flexible supermolecules in a solvent environment.

Further, we have set the stage to model transition states (the tetrahedral intermediates) of the catalyzed thiolysis reaction for various substrates. Beyond the initial complexation step we will then consider kinetic aspects of molecular recognition in these artificial enzymes.

Acknowledgment. This work was supported by a grant from the Ministère de la recherche et de l'enseignement superieur. We are very indebted to Drs. C. Sirlin and J. Holmes for reading the manuscript. P.A.K. is pleased to acknowledge support from the National Institutes of Health through Grant GM-29072. G.W. and P.A.K. acknowledge travel support through NATO Grant 0478/82.

(60) Hayes, D. M.; Kollman, P. A. *Catalysis in Chemistry and Biochemistry. Theory and Experiment*; Pullman, B., Ed.; Reidel, D. Publishing Co.: 1979; pp 77–90. Alagona, G.; Desmeules, P.; Ghio, C.; Kollman, P. A. *J. Am. Chem. Soc.* **1984**, *106*, 3623–3632.